Chapter 12

Radio Frequency Magnetron Sputter Deposition as a Tool for Surface Modification of Medical Implants

Roman Surmenev, Alina Vladescu,
Maria Surmeneva, Anna Ivanova, Mariana Braic,
Irina Grubova and Cosmin Mihai Cotrut

Additional information is available at the end of the chapter

http://dx.doi.org/10.5772/66396

Abstract

The resent advances in radio frequency (RF)-magnetron sputtering of hydroxyapatite films are reviewed and challenges posed. The principles underlying RF-magnetron sputtering used to prepare calcium phosphate-based, mainly hydroxyapatite coatings, are discussed in this chapter. The fundamental characteristic of the RF-magnetron sputtering is an energy input into the growing film. In order to tailor the film properties, one has to adjust the energy input into the substrate depending on the desired film properties. The effect of different deposition control parameters, such as deposition time, substrate temperature, and substrate biasing on the hydroxyapatite (HA) film properties is discussed.

Keywords: Hydroxyapatite, magnetron sputtering, corrosion resistance, cell viability

1. Introduction

It is well known that the long-term success of the dental and orthopedic implants is determined by a good osseointegration, which can be guaranteed by a good connection between the bone cell and implant. This connection is dependent on the phenomena which can take place immediately after insertion of the implant in human body. The first process after implantation is the interface between implant and the proteins, by formatting a thin layer which will act as a mediator of a good proliferation of the cells. Thus, protein adsorption determines the nature of the interface between the bone and implant, which will stimulate a fast cell growth, leading to a rapid osseointegration of the implant. In the past few years, it was demonstrated that the osseointegration of the metallic implants could be increased by coating the implant surface

with bioactive coatings, which proved to accelerate the bone bonding rate. It was certified by World Biomaterial Congress in 2008 and 2012 and 2016 that this topic is one of the major topics in biomaterials.

Various different techniques are currently available for deposition of calcium phosphate (CaP), in particular hydroxyapatite (HA) coating, to metallic materials, including plasma spraying, pulsed laser deposition, biomimetic crystallization methods, electrophoretic deposition, sol-gel deposition, magnetron sputtering, etc. [1].

Among the listed methods, plasma spraying is the only approach which is commercially approved for HA coatings deposition on metal implants by the food and drug administration (FDA) [1]. The method is based on the formation of a condensed layer of individual particles deposited on a metal substrate. The particles originating from a powder material are carried by a gas stream and passed through electrical plasma produced by a low voltage, high current electrical discharge. During this process, the heated particles crystallize and agglomerate during film formation. The coating features are determined by the chemical and mechanical properties of the used powder material, by the distance between a source and a substrate, the current of the electric arc, the deposition rate, and the work gas composition. Plasma spraying allows to produce coatings up to 300 μm in thickness. This technique has some significant limitations: poor uniformity in coating thickness and adherence to substrate, low crystallinity, poor mechanical properties on tensile strength, wear resistance, hardness, toughness, and fatigue [2]. Furthermore, plasma spraying does not allow to produce an uniform HA coating on substrates with complex geometry. Meanwhile, the most important disadvantages of this method are considered to be the presence of impurity phases. A higher temperature (6,000–10,000°C) is used during plasma spraying, the crystal structure of the HA powder can be easily destabilized and decomposition into mixture of HA, CaO, tricalcium phosphate, and tetracalcium phosphate, and a considerable amount of amorphous phases is occurs [3]. Structural inhomogeneity can lead to differences in coating resorption [3] and a reduction in coating-substrate interfacial strength [4, 5]. The alternative coating approaches have been extensively developed and tested to overcome the weaknesses of plasma spraying, namely sol-gel deposition and RF-magnetron sputtering. An overview of these three techniques is given in **Table 1.**

Sol-gel deposition is a widespread method to produce CaP coatings [6, 7]. This method is based on the preparation of a suspension (sol) in the dispersion phase with its subsequent transition into a gel and the treatment of a metal surface with the resulting colloid. Thermal treatment at the coating material's crystallization temperature is required as the final step. The method makes it possible to produce a dense CaP coating with the thickness of 0.5–30 μm. Sol-gel deposition is a relatively inexpensive technique compared to others. The method has the potential to coat implant with complex shape by using simple setup [8]. Furthermore, it has the benefits of phase and structural uniformity [9, 10]. However, too low processing temperature leads to an amorphous or a nanocrystalline coating structure and requires, therefore, additional annealing of the coating to increase the degree of crystallinity. The major advantages of sol-gel method are good mechanical properties, corrosion resistance, and adhesion strength due to their nanocrystalline structure [11, 12]. However, the sol-gel deposition has disadvantages such as high permeability, low wear-resistance, and difficult porosity control, which hinders its commercial

http://dx.doi.org/10.5772/66396

Technique	Thickness (μm)	Advantages	Disadvantages	Ref.
Plasma spraying	~30–300	High deposition rate; sufficiently low cost; coatings usually have microrough surface and porosity	Poor adhesion; low crystallinity, poor mechanical properties on tensile strength, wear resistance, hardness, toughness and fatigue; high temperatures induce structural inhomogeneity and HA decomposition; rapid cooling produces cracks in coatings	[2–5]
Sol-gel coating	~0.5–30	Inexpensive; low processing temperatures; high purity; fairly good adhesion (40 MPa); can coat complex substrates; high phase and structural uniformity	Requires high sintering temperatures; poor control of chemical and phase composition; high permeability; low wear-resistance; difficult porosity control	[6–14]
RF-magnetron sputtering	~0.04–3.5	Uniform coating thickness; dense pore-free coating; ability to coat heat-sensitive substrates and with complex structure; high-purity films; ability to control the coating structure and the Ca/P ratio; good adhesion (30 MPa)	Line-of-sight method; low deposition rate; expensive	[2, 3, 6–9, 15, 16]

Table 1. The advantages and disadvantages of the most applied methods for HA coating deposition.

application [13]. Meanwhile, annealing can lead to a deterioration of the coating's adhesion. Furthermore, adsorbed organics within the sol-gel process can also cause coating failure.

Despite all the advantages of the above-described methods, their most essential limitation is the difficulty to control the phase and chemical composition of a CaP coating. In its turn, RF-magnetron sputtering allows to control the properties of CaP films within a rather wide range and to form a dense, uniform coating to devices with complex configurations with high adhesion and with uniformity in thickness and composition [17–24].

This high flexibility makes RF-magnetron sputtering, however, a rather complex method, especially for the deposition of multicomponent materials such as calcium phosphates. There are many process parameters that can have a direct effect on the coating's characteristics. For example, the coating composition can be influenced by the target composition and sputtering parameters such as gas pressure, substrate bias, and the deposition temperature. During

RF-magnetron sputtering, the dense plasma interacts strongly with the substrate [25], which causes an intense ion bombardment of the growing coating. The energetic particle bombardment may determine the growth film. During the RF discharge, the positive ions are accelerated and bombard the substrate with high energies, which are dependent on the discharge excitation frequency. It is plausible that the plasma density is higher in front of the substrate opposite to the plasma torus above the erosion racetrack. Under target erosion zone, the bombardment of the substrate surface by high energetic oxygen species (O^-) occurs, which was confirmed by a number of authors [26–30]. These ions are generated at the target surface, accelerated in the cathode dark space and move with a high energy perpendicular from the target toward the substrate surface [31–33]. Cai et al. [34] described the effect of a local change in the growth rate of ZnO coating in the region of the target erosion zone which is connected with the sputtering of the coating with negatively charged ions. So, the Ar^+ and O^- bombardment is the major part of the energetic particle bombardment occurring in RF discharges. It plays an important role during the film deposition in RF sputtering, because the temperature of the substrate may increase with increasing discharge power. The properties of the RF-magnetron sputter-deposited films are highly influenced by the bombardment of the growing film with species from the sputtering target and from the plasma. The latter is determined by the deposition parameters such as the working gas pressure and composition, target-substrate distance, and substrate bias voltage. Different energetic and thermal circumstances may result in a different final quality and structure of the applied coating. Control of these parameters is essential to modify the HA coating structural properties, its composition, and mechanical characteristics.

This chapter reports on the influence of discharge RF-power, substrate temperature, and spatial sample arrangement regarding the target erosion zone on the properties of the CaP films, its mechanical properties, and behavior *in vitro*.

2. Literature overview of RF-magnetron sputtering of CaP coating and its comparison with chemical method

2.1. Principles of RF-magnetron sputtering

A magnetron sputtering system is a technological equipment which allows depositing thin films by sputtering of a target material in a magnetron discharge plasma. This type of system is based on the formation of electric and magnetic fields perpendicular to each other in the near-cathode region. By supplying a voltage between the cathode and the anode, a glow discharge is ignited. When the voltage is applied, the free electrons are repelled from the cathode or target and collide with the atoms of the working gas, creating ions, and new electrons. The positive ions are accelerated toward the target. The collision of the positive, energetic ions with the target leads to its sputtering. Particles removed from the target surface are transported to the substrate and the chamber walls. Not only atoms but also emission of electrons occurs due to the interaction of the ion flux with the target surface. The amount of emitted electrons to each approaching ion is known as the secondary electron emission yield and depends on the properties of the target material, the energy, and the type of bombard-

http://dx.doi.org/10.5772/66396

ing particles. Secondary electrons are necessary for the ionization of the working gas and the maintenance of the discharge.

The magnetic field holds electrons in immediate proximity to the target in a so-called electron "trap" that is created by the intersecting electric and magnetic fields. The electrons oscillate in this trap until several ionizing collisions with atoms of the working gas occur. The plasma is localized above the target surface, due to the presence of the magnetic field. Hence, the target surface is sputtered in areas located between the magnets of the magnetic system. As a result, an erosion zone (racetrack) is created in the form of a closed-loop path with a shape determined by the magnetic system.

The RF plasma is conducted by electron ionization, which exhibited an oscillating movement at the RF-magnetron frequency of 13.56 MHz. At this frequency, the ions could not pursue these oscillations due to their mechanical inertia. This excitation is much more effective than the ionization by nonoscillating secondary electrons, leading to decrease of the voltage of the RF discharge. During the positive half-cycle, the target acts not as a cathode but as an anode. Therefore, the plasma density in front of the substrate is significantly higher for RF. **Figure 1** shows the potential distributions, in which the positive ions (Ar^+, O^+, and Ca^+) are accelerated in the cathode fall V_p-V_{dc} and the target sputtering will take place. At the same time, the electrons and negative ions (O^-) were moved from the target to the substrate, which along to the reflected neutral argon atoms will arrive at the substrate and perform the growth of the coating. In **Figure 2**, the effects of energetic particles on a solid surface during ion-assisted growth during the RF discharge are shown. The secondary and back-scattered electrons, as well as the reflected ions and neutrals, cause a higher plasma density in front of the substrate for RF excitation and hence a higher ion saturation current to the growing film.

It can be seen that the electrons are kept out of the substrate and only those, which have a sufficiently high energy, will be able to pass through the potential barrier and arrive to the substrate, even if they have a low current. Both neutral species and high-energy negative ions (i.e., O^-) are capable of striking the substrate.

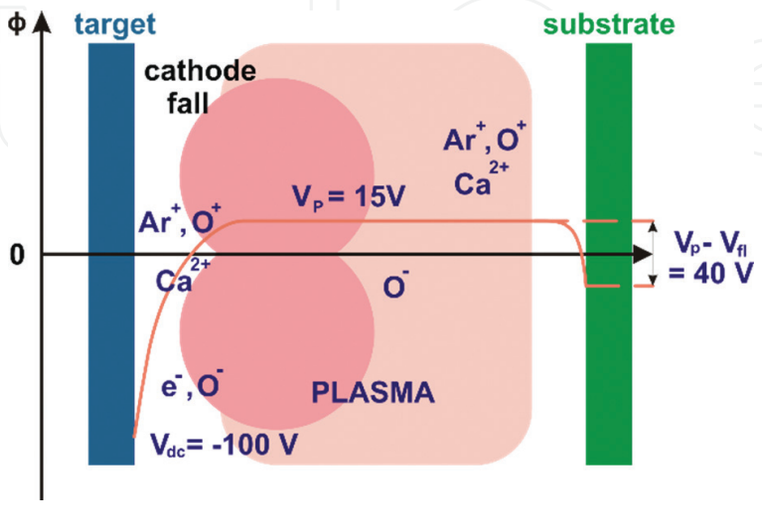

Figure 1. Potential distribution in a magnetron sputtering discharge, excited by RF.

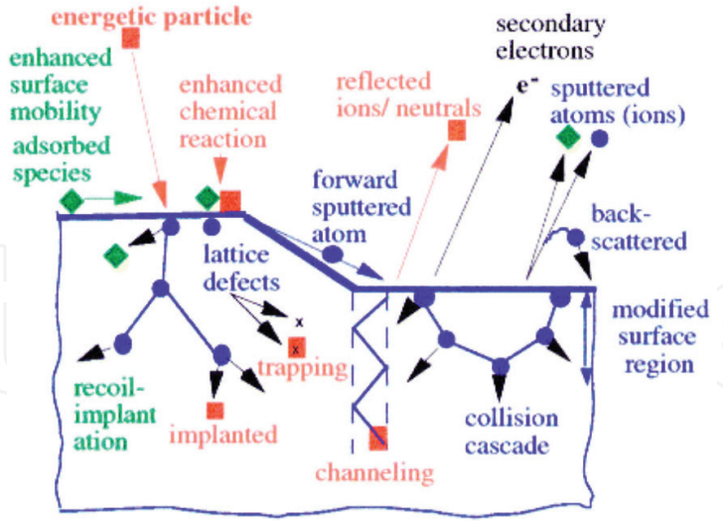

Figure 2. The effects of energetic particles on a solid surface during ion assisted growth [35].

The properties of the RF-magnetron sputter-deposited films are highly influenced by the bombardment of the growing film with species from the sputtering target and from the plasma. The latter is determined by the deposition parameters such as the working gas pressure and composition, target-substrate distance, and substrate bias voltage. Control of these parameters is essential to modify the HA coating structural properties, its composition and mechanical characteristics. The thermal and energetic conditions at the substrate surface influenced by the different plasma species determine the elementary processes (adsorption, diffusion, and chemical reactions) as well as the microstructure and stoichiometry of the film growth. The energy available per incoming particle and ion-to-atom ratio is, therefore, essential in plasma processing of solid surfaces in the case of thin film growth. Functional properties of the thin films are largely determined by the intrinsic coating features, which defined not only by the material properties but, to a large extend, also by the thin film growth mechanism. Passing through several stages, adsorption, nucleation growth, and increase film thickness, a defined coating structure is formed. The extended structure zone model identifies the evolution of a polycrystalline thin film and its relation with the deposition conditions.

2.2. Morphology of RF-magnetron sputtering of CaP coating

The surface morphology of the HA coatings appears to play a significant role in implant-tissue interaction and osseointegration [1]. RF-magnetron sputtering allows to deposit dense, uniform coating, without apparent defects (cracks, gas bubbles, and others) keeping the initial substrate topography [1, 36]. The latter is beneficial in case of porous scaffolds and other substrates with the complex structure. Meanwhile, it is well known that the coating surface morphology is connected to their growth mechanisms. In this way, it varies according to the deposition process conditions. Most often CaP coatings produced by RF-magnetron sputtering at room temperature possess a low crystalline or amorphous structure. It occurs due to the energy flux arriving the substrate at the applied process conditions that is not high enough to ensure crystalline coating formation on the unheated substrate holder. To induce the crystal-

http://dx.doi.org/10.5772/66396

linity of the coatings and transform the amorphous calcium phosphate into HA, the thermal treatment at $T > 500°C$ (*in situ* and *ex situ*) is applied [37–42].

The surface morphology of the coatings to be shown strongly depends on the substrate temperature. Bramowicz et al. [43] performed the deposition on silicon substrates with the temperature varied in the range of 400–800°C (**Figure 3**). The sample deposited at 400°C was observed to exhibit some circular cavities. At the increase of the deposition temperature, the cavities started to overlap, leading to the formation of uniform grains with comparable size. At 500°C, a threshold in the growth mode was observed, as the predominant morphology (cavities in otherwise flat surface) turned into a series of convex grains with well-developed grain boundaries. The authors concluded that the deposited HA coatings exhibit bifractal behavior, their surface topography can be thought of as two interpenetrating spatial structures with different characteristic length scales (cavities and clusters of cavities), which independently evolve with the deposition temperature.

The change of the routine of the coating preparation by adjusting the process parameters, such as substrate-target distance, working gas pressure, bias potential on substrate holder, ensuring higher energy flux arriving at the substrate allow to obtain crystalline coating at room temperature [44–47]. López et al. [44] published a study on the control of the thermodynamic properties of the plasma to form a coating with higher crystallinity. The authors modified the sputtering geometry by positioning two magnetrons face-to-face with a substrate holder kept in a floating electric potential positioned at a right angle to the magnetrons (off-axis). It was shown that at an RF-power density of 24 W/cm^2 after 180 min of sputtering, the transformation of amorphous phase in the coating to the crystalline one occurred. Surmeneva et al. [48] in their work deposited higher crystalline coatings by sputtering a Si-containing HA target using a setup with an RF-magnetron source (5.28 MHz) at an RF-power density of 0.5 W/cm^2 and a target-substrate distance of 40 mm. The experiments were performed with a grounded substrate holder (bias 0 V) and a bias voltage of -50 or -100 V. The temperature of the substrate

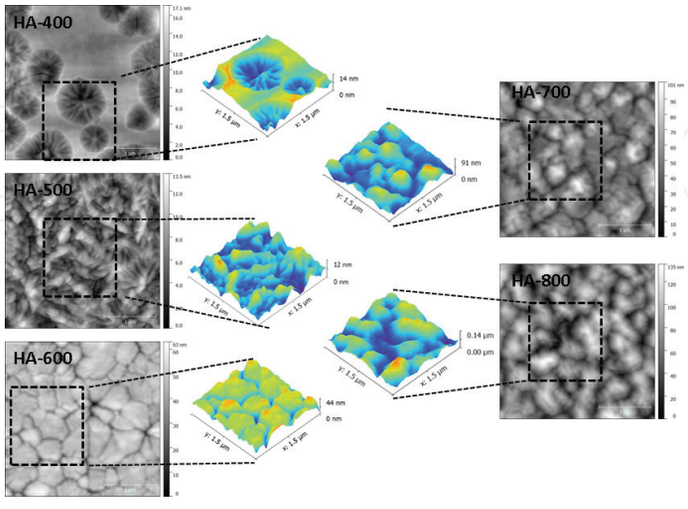

Figure 3. 10 × 10 μm, 2 planar AFM images of residual surfaces of the HA substrate on Si substrate deposited at: (A) 400°C, (B) 500°C, (C) 600°C, (D) 700°C, and (E) 800°C. Insets: 3D projections of marked areas to show changes in surface morphology [43].

during deposition reached 200°C due to heating by plasma. The effect of ion bombardment on the morphology and microstructure modification of Si-HA coatings is shown in **Figure 4**. The typical surface morphology of the HA coatings deposited on a flat silicon grounded substrate consisted of mound-shape grains (**Figure 4a**). By applying a substrate bias a distinct decrease in the morphological features dimension was observed. The coating cross-section structure was studied by SEM. The samples were prepared by the chemical etching of one half of the coating in 1 M aqueous HCl. The etched regions of the coating are shown in **Figure 4** (right side). The SEM study showed that the coatings deposited on the grounded substrate consisted of dense columnar grains grown perpendicular to the substrate surface. The columnar structure is the typical characteristic of films deposited by means of magnetron sputtering. The physical reason for the phenomenon of this structure is explained by Krug [49] and Bales and Zangwill [50] as a shadowing effect which can occur if adatoms impinge on the substrate under an angle which deviates from the substrate normal. With negative bias, the columnar structure was completely replaced by a very fine equiaxed grain structure which is reflected in the surface morphology. Therefore, it is considered that due to applying the negative bias, the particles arriving on the growing film have higher enough energy to disrupt column growth and force renucleation. Moreover, an increased ion bombardment may induce coating resputtering effect resulting in flat surface morphology. Thereby, the HA coatings can be deposited by RF-magnetron sputtering in such a way to control the coating morphology.

2.3. Composition of RF-magnetron sputtering of CaP coating

The thermodynamic stability, reactivity, solubility, and mechanical properties of CaPs were reported to strongly depend on the Ca/P ratio [4]. The calcium phosphate with low Ca/P ratio proves to have high dissolution rate. When the Ca/P ratio is equal to 1.67, the stoichiometric compound is obtained, which is referred as hydroxyapatite (HA). In biomedical applications,

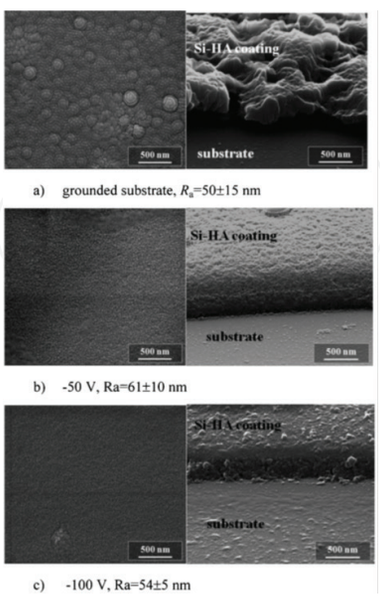

Figure 4. SEM images of the Si substrate coated with HA coating at the grounded substrate holder (a) 0 V, (b) −50 and (c) −100 V. Left: top view; right: side view after etching. The R_a was measured before etching [48].

http://dx.doi.org/10.5772/66396

this compound is the most desired to obtain because the Ca/P ratio is close to that of natural bone. Thus, the Ca/P ratio is one of the main characteristics of a biocompatible film and it depends on the applied deposition control parameters such as RF-power, substrate bias, working gas pressure, and configuration of the samples in the vacuum chamber [51]. It is shown that the ratio of elements in the deposited coating may differ substantially from their ratio in the target [24, 28, 52]. It was reported that when sputtering from multicomponent ceramic targets, such as superconducting oxides, HA, and other CaP materials, the alteration in coating composition may occur due to the preferential sputtering, which can initially cause the stoichiometry of the film to deviate from that of the target. However, at steady state, the composition of the sputtered flux must be the same as the target composition unless extensive diffusion occurs in the target [53]. It was also reported that at least 1000 Å (or more of the multicomponent target) need to be removed before the coating would reflect the stoichiometry of the bulk target [54]. Thus, the composition of the coating may be quite different from that of the target material, depending on the type of sputtering system, and parameters used for deposition.

Figure 5 shows the typical spectra for the fitted high resolution XPS obtained for O1s, Ca2p, and P2p regions of CaP films deposited by RF-magnetron sputtering onto titanium substrates. For the studied CaP coating, the O1s envelope (**Figure 5a**) was fitted with energy O1s = 531.9 eV of the calcium in the structure of HA. The energy of $Ca2p_{3/2}$ = 347.1 eV (**Figure 5b**) was established for all Ca-O bindings. Finally, the P2p was fitted with two binding energies for the $P2p_{3/2}$ peak (**Figure 5c**): (i) the $P2p_{3/2}$ = 132.9 eV was established to the phosphorous bonded to the oxygen in the $(PO_4)^{3-}$—groups in the hydroxyapatite structure and (ii) the $P2p_{3/2}$ = 133.8 eV was attributed to the P-O bindings in the calcium phosphate phase. For nanocrystalline HA coatings deposited via the RF-magnetron sputtering the ratio of Ca/P was reported in the range between 1.6 and 2.9 [47, 55]. The optimum Ca/P ratio was reported to be in the range of 1.67–1.76 [4].

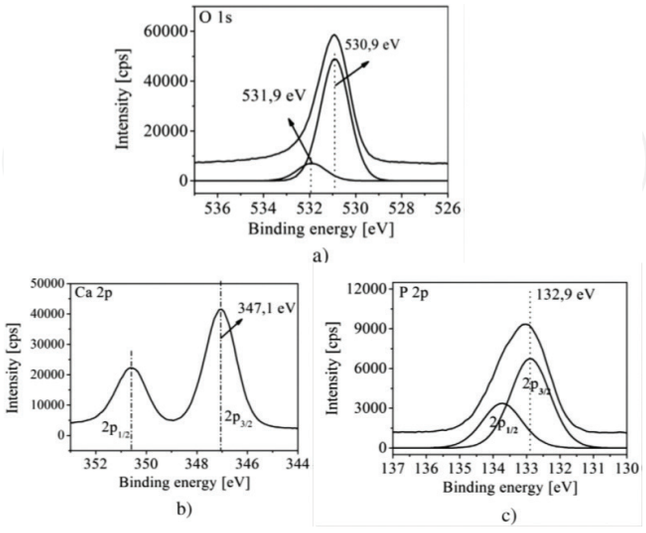

Figure 5. XPS: (a) O 1s, (b) Ca 2p, and (c) P 2p spectra of the CaP coating deposited via RF magnetron sputtering onto a titanium substrate [56].

At the low deposition temperature an amorphous coating structure was obtained; the increase of the deposition temperature leads to the Ca/P ratio change in the range of 1.41–1.69 [43]. It was demonstrated that the Ca/P ratio achieved the value of 1.63–1.69 for samples prepared at temperatures between 600 and 800°C. It was found that the Ca/P ratio of the coating is different than that of the target, due to specific target sputtering mechanisms. Moreover, it was reported that P ions are pumped away before reaching the substrate [17]. In the present case, at relatively low deposition temperature, the deposition conditions yielded Ca-deficient films, whereas temperature increase resulted in stoichiometric HA films. Possible phenomena causing these results include differences in sticking and removal rates of atoms on the growth surface and gas scattering phenomena [53]. Film growth at relatively high temperatures implies that the sticking probability of the incoming species can be less than unity, which in the case of compound growth can result in modified film composition.

An increase of the negative bias applied to the substrate led to the increase of the coating crystallinity and of Ca/P ratio from 1.53 to 3.88 [52, 55, 56]. Feddes et al. [57] explained this phenomenon by assuming that phosphorus was resputtered from the growing film surface by ion bombardment with the energy determined by the potential drop in the cathode dark sheath. The authors of the study reported that calcium was carried by positively charged radicals (e.g., CaO^{+}) and ions (e.g., Ca^{+} and Ca^{2+}) generated in the plasma [57]. Moreover, it is explained that higher negative substrate biasing resulted in higher fluxes of CaO^{+} cations onto the surface and it became more difficult for $(PO_4)^{3-}$ anions to reach the surface, which explained the higher Ca/P ratios at higher negative biases [48].

The composition of the CaP coatings may be controlled by the RF-magnetron sputtering and may be changed by deposition temperature. The increase of the deposition temperature leads

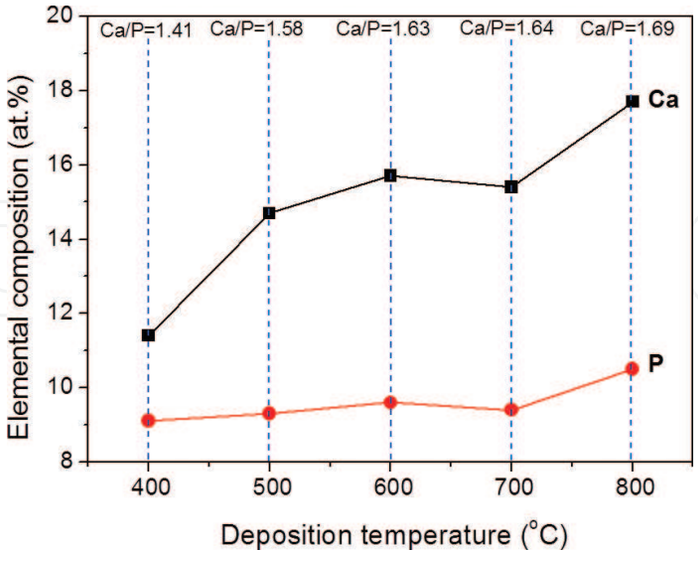

Figure 6. Elemental composition determined by XPS of the CaP coating deposited via RF magnetron sputtering at different deposition temperature onto a silicon substrate [43].

http://dx.doi.org/10.5772/66396

to the Ca/P ratio change in the range 1.41–1.69 [43]. The deposition temperatures influence the Ca/P ratio, which achieves 1.63–1.69, that is very close to the stoichiometric HA (Ca/P = 1.67), for samples prepared at temperatures between 600 and 800°C (**Figure 6**).

2.4. Water addition into an working gas atmosphere effect of RF-magnetron sputtering of CaP coating

A similar trend was observed for the coatings deposited in H_2O-containing atmosphere by Ivanova et al. [28] (see **Figure 7**). The Ca/P ratio varied within the range of 1.53–1.70, and first increased with the distance from the center of the substrate holder. The highest Ca/P ratio was obtained for the samples exposed above the racetrack. Feddes et al. [57] reported that the P ions can be resputtered by negatively charged oxygen ions, leading to the variation of the Ca/P. Also Takayangi et al. [58] found that the high-energy negative ions appear in the erosion area of the oxidized cathode due to a large amount of electrons which are trapped by magnetic field within this zone. So, the negative oxygen ions formed as well as Ar ion bombardment of the growing HA film caused its stoichiometric deviation from the target composition. So, the RF-magnetron sputtering is well-suited method to prepare coatings with different Ca/P molar ratios by variation of the substrate temperature, substrate bias, and position of the sample with regard to the target erosion zone [48].

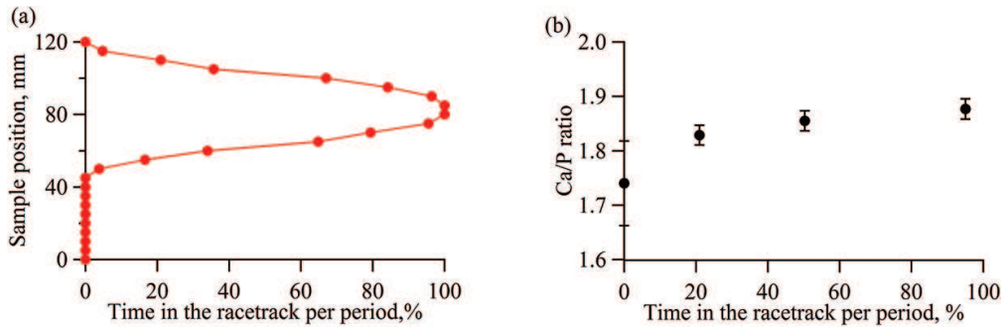

Figure 7. The relation between the sample positions on the substrate holder: (a) and a Ca/P ratio, (b) as function of the time in the race track per period [28].

2.5. Microstructure of RF-magnetron sputtering of CaP coating

At the low energy flux into the substrate, the amorphous HA coating is growing [59]. Thus, the deposition temperature of the HA coating plays an important role to the formation of the crystalline structure, which influence many other properties of the coatings. **Figure 8** shows the evolution of the crystallinity on the deposition temperature. At low temperature, the CaP coating shows only two peaks: (002) and (202). As the deposition temperature increased, more peaks are seen, the (200), (222), (213), and (004) planes) indicating the formation of the crystalline structure. The grain sizes, calculated by the Scherrer formula, increase with the deposition temperature, resulting in crystallites aggregation due to the higher adatoms mobility.

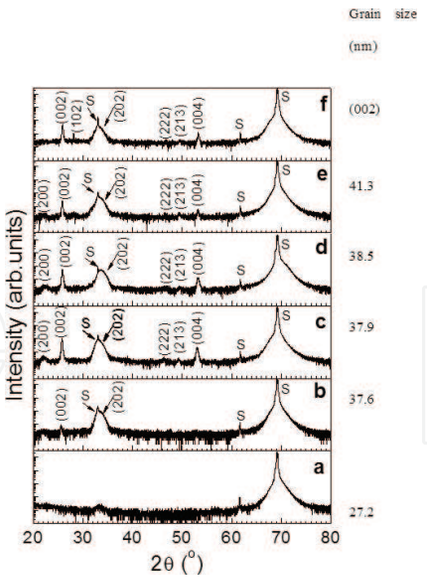

Figure 8. XRD spectra of the CaP coatings deposited at different deposition temperature [59].

The phase composition and structure of the CaP coating depend on the process conditions as it was mentioned above. RF-magnetron sputtering allows to deposit the CaP coatings of either amorphous or crystalline structure of a certain phase composition that along with the Ca/P ratio influences the coating behavior *in vitro* and *in vivo* [60]. The high dissolution rates of the amorphous lead to long-term stability reduction of the implanted devises. With the aim to maintain the HA coating integrity the researchers apply the postdeposition or *in situ* annealing of the films. Several authors reported that the transition from amorphous to crystalline coatings can be controlled by the heat-treatment temperatures and heating environment (air

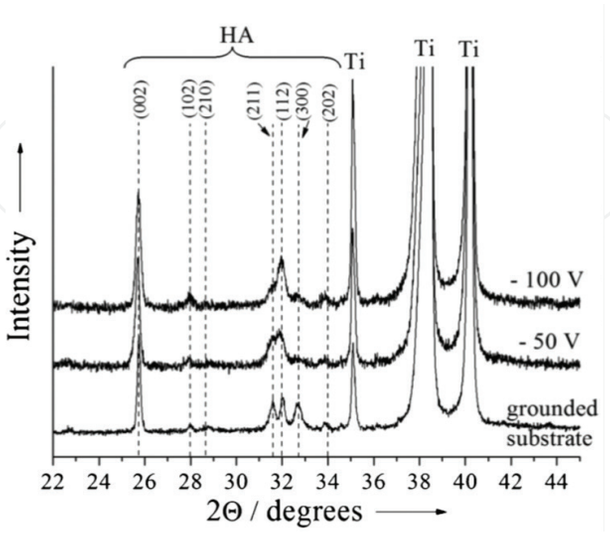

Figure 9. XRD spectra show variations of the intensity distributions, revealing that the studied samples have a different texture [48].

http://dx.doi.org/10.5772/66396

and water vapor) [61–63]. Meanwhile, crystalline coating can be obtained by turning the energy of the bombarding ions or ion to atom ratio arriving the substrate through manipulation with the substrate bias, working gas composition, pressure, and target-substrate distance.

The influence of the substrate bias voltage on the structure of the Si-containing HA coating was studied by Surmeneva et al. [48]. The X-ray diffractograms of the deposited coatings consisted of the reflexes corresponding well to the expected Bragg peaks for hydroxyapatite (ICDD PDF No. 9-432) (**Figure 9**). With a grounded substrate, the strongest peak of the Si-HA coating was the reflection from the (002) plan resolved at 25.9°. Thus, crystallites of Si-HA preferentially grew in the (002) crystallographic orientation perpendicular to the substrate surface. With an increase in the substrate bias voltage to −100 V, the intensity of the (002) peak relative to the other peaks was observed to decrease. The XRD pattern of the coating at negative bias showed broad overlapping peaks around 32°, which indicates the decrease of the crystallite size or/and the presence of the microstress in the film. The average crystallite size as determined by the Scherrer formula was 70 nm for the coating obtained on a grounded substrate (0 V) and 45 nm for the coatings deposited at negative bias (−50 and −100 V). Thus, the enhancement of the energy of the bombarding ions reduces the texture of the film and the crystallite dimension.

The crystalline HA coatings were obtained by RF-magnetron sputter deposition in water containing atmosphere [28]. It was shown that the HA coatings exhibited considerable change on preferential orientation while the samples approach the target erosion zone. According to XRD analysis with shifting the sample radially from the center of the substrate holder the texture coefficient of (002) peak decreases while the (300) peak grows up. **Figure 10** shows detailed highlights from the two ultimate cases of the deposited HA coatings preferentially oriented in the (002) and (300) directions. The structural features of

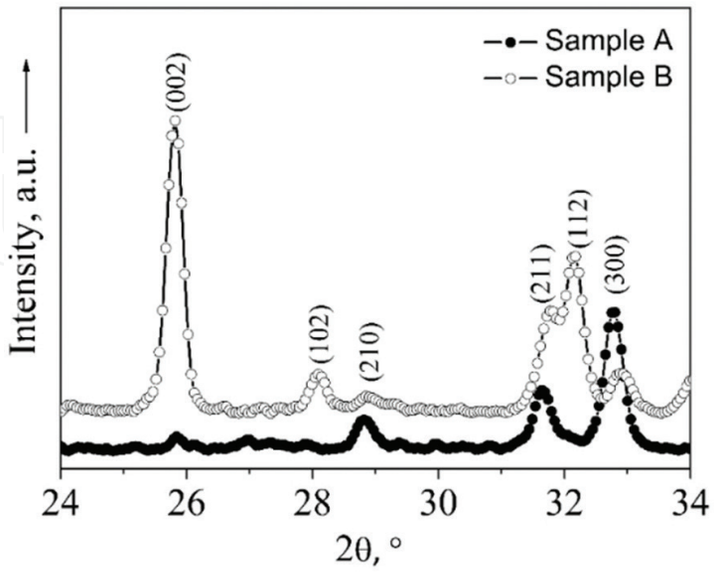

Figure 10. Highlights from X-ray diffractograms of HA films deposited under racetrack (Sample A) and in the centre of the substrate holder (Sample B).

the films were quantitatively studied. The lattice parameters (*a*, *b*, and *c*) of the measured samples were revealed to be higher than that of the bulk HA. The (002) textured coating (Sample B) is characterized by $a = 9.410$ Å and $c = 6.934$ Å; the (300) textured film (Sample A) is with a = 9.490 Å and $c = 6.925$ Å. This behavior is commonly observed in physical vapor deposited thin films and is attributed to the compressive stress arising in the film within growth and the stoichiometric imbalance of the film composition. In this way, the deposition conditions which were realized under the racetrack lead to the transformation of the HA film orientation. It is considered that the texture change is resulted by high energy ion bombardment of the growing film deposited under the target erosion zone. This not only affects the deposition rate but also influences the structure and functional properties of the film.

The development of microstructure in the trend of the coating growth was also studied with the help of TEM cross-section images. **Figure 11** shows the cross-sectional bright and dark fields of a 250-nm thick CaP layer prepared by FIB. Note that the coatings had a gradient structure with a nanocrystalline layer at the interface. This result is in good agreement with the results published in reference [48]. The first columnar structure nucleated perpendicular to the interface, within the range of 30–50 nm from the interface between the coating and substrate. The CaP film is well defined, dense, and homogenous. In the dark-field images, the columns have a lateral size of about 40 nm. In **Figure 11a**, the clear structure of HA, with reflections from (100), (002), (211), and (200) planes, was seen. Based on TEM, the average crystal size of the top CaP layer was 30 ± 20 nm. The crystals showed a perfect crystalline structure, being in concordance with the value obtained from the XRD spectra (40 nm).

Also in **Figure 11**, the polycrystalline structure of the HA coating can be observed. Both ED patterns and d-spacing values (1.90, 2.12, 2.25, 2.82, 3.19, 3.43, 4.10, and 8.20 Å) confirmed that the deposited coatings possess the structure of HA and the absence of other crystalline phases. The physical reason for the phenomenon of this structure is explained by the authors of the study [64] as a shadowing effect which can occur if adatoms impinge on the substrate under an angle which deviates from the substrate normal. The microstructure evolution of the thin film can be described with the structure, zone model (SZM), which characterizes the

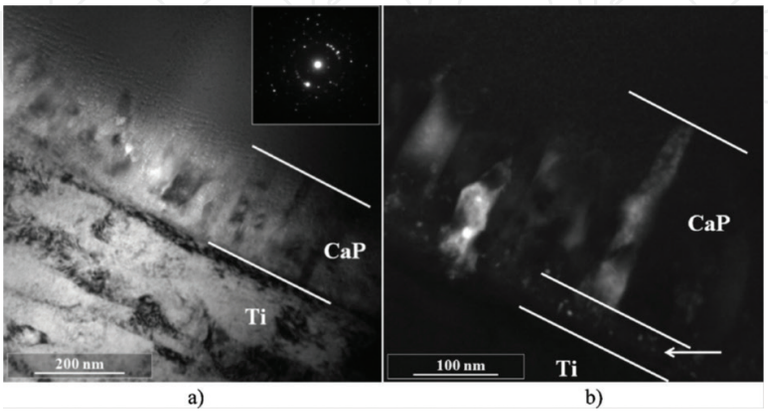

Figure 11. Cross-sectional bright field: (a) and dark field, (b) TEM images of a 250 nm thick CaP layer were prepared by FIB. The electron diffraction pattern (insert left image) reveals the presence of a polycrystalline phase [52].

microstructure and texture as a function of the deposition parameters. A good overview of an SZM is given by Mahieu et al. [65–67] developed the extended structure zone model (ESZM) that explains the transformation of the texture and microstructure of thin films as a function of adatom mobility.

The texture change occurred in thin films during their growth is a fundamental issue. It can be determined with the help of several factors, such as precursor adatoms sticking probability, adatom diffusion on the surface, and interaction of high-energy particles with the surface of the growing film. In the HA structure, the (002) plane has the lowest surface energy [68]. For this reason, to minimize the surface energy, the HA coatings grow on (002) orientation. In the literature, it was reported that the preferred (002) orientation can be thermodynamically changed by increasing oxygen ions bombardment in the deposition process [66]. For example, Van Steenberge et al. [69] demonstrated that the preferential orientation of the CeO_2 films prepared using the reactive magnetron sputtering method can be controlled by increasing oxygen flow. The influence of different crystalline planes during the collision anisotropy can also be treated as an explanation of the obtained results. The (002) plane of hexagonal structure is the most closely packed and it can be easily damaged by severe bombardment of ions accelerated in the cathode racetrack giving rise to loosely packed (100) plane [70, 71]. This finding is important, because crystallographic texture of polycrystalline thin film is one of the essential microstructural features, which is responsible for its properties. In hexagonal HA, a, b, and c planes exhibit anisotropy in mechanical properties, resolvability, biocompatibility, and absorption ability [72–75]. Naturally occurring apatite crystals frequently exhibit preferred orientations resulting from highly specific biological processes and these preferred orientations are believed to affect the biological and biomechanical performance of hard tissue [73, 76, 77]. Moreover, recent investigations suggest that HA with textured in a tailored manner surfaces may enable a new level of control over cellular behavior due to of protein adsorption anisotropy on the different faces of hexagonal HA crystals. Molecular modeling and *in vitro* analysis have shown that acidic bone proteins and other proteins exhibited high affinity to the (100) plane of HA [55]. Moreover, adsorption-desorption of the protein on nanosurface plays an important role in cell adhesion and mineralization of biomaterials. Thus, by controlling the preferential orientation of sputtered HA coatings, the behavior of the coatings in human body can be tailored, assuring their successful for biomedical applications.

2.6. Electrochemical *in vitro* tests of RF-magnetron sputtering of CaP coating

After implantation in human body, any metallic biomaterials are affected by the action of the body fluids [60]. The metallic biomaterials are degraded by corrosion processes, which disturb the normal body system, leading in the end at the rejection of the implant. For this reason, before the preparation of new biomaterial, it is important to know the effect of the corrosive solutions on its characteristics. In the case of the coatings, the corrosion resistance can be controlled by the adjustment of deposition parameters. The corrosion behavior of the biomaterials at the contact with simulated body solutions (saliva, SBF, PBS, and 0.9% NaCl, etc.) can be evaluated by various techniques; the most used being the potentiodynamic polarization method. The corrosion behavior of hydroxyapatite is influenced by the many factors such as composition, crystallinity, compactness, and porosity,

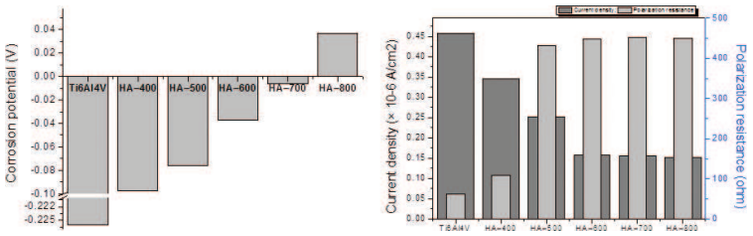

Figure 12. Evolution of corrosion potential, corrosion current density, and polarization resistance on the deposition temperature of the sputtered hydroxyapatite coatings in Fusayama artificial saliva solution (pH = 5) at 37°C [59].

which are depended on the deposition parameters. For example, Ducheyne et al. found that the stoichiometric hydroxyapatite coatings (Ca/P = 1.67) exhibited low dissolution rate than other types of calcium phosphates [78].

In a previous paper, we demonstrated that the deposition temperature is one of the factors which can affect the corrosion resistance of sputtered hydroxyapatite coatings as following [59]. The increase of the deposition temperature from 400 to 600°C leads to the decrease of the corrosion current density and increase of the polarization resistance (**Figure 12**), indicating an improvement of the corrosion resistance. For further increase of deposition temperature from 600 to 800°C, the corrosion current density and polarization resistance were not affected (**Figure 12**). Comparing the values of corrosion potentials, all the coatings presented more electropositive values than the uncoated Ti alloy (**Figure 12**), demonstrating that the coatings are a good solution for improving corrosion resistance of the Ti6Al4V alloy. The increase of the deposition temperature tends toward more electropositive values for hydroxyapatite, indicating also an enhancement of the corrosion resistance. In the literature, it is commonly admitted that a material is resistant to the corrosion when exhibited more electropositive values for corrosion potential, low values for corrosion current density and high ones for polarization resistance [79, 80]. If we take into account these criteria, it can be observed that the hydroxyapatite prepared between the 600 and 800°C has the best resistance in Fusayama artificial saliva solution (pH = 5) at 37°C, being proper for the dental applications. This results was accounted to the differences in the composition of the samples, the EDS measurements showing that HA-400 is nonstoichiometric (Ca/P = 1.80) while the HA-600, HA-700, and HA-800 exhibited Ca/P ratio closed to 1.67 [59].

2.7. Mechanical properties of RF-magnetron sputtering of CaP coating

To assure the success on long term of the metallic implants coated with HA, the coated surface should exhibit a high hardness, low friction performance and superior bonding strength to the metallic surfaces in order to support potential fatigue stress at the time of surgical procedure or after implantation. Altering the metallic surface texture, namely, the implant roughness, via different pretreatment techniques or/and their combination is the most common used and relatively inexpensive way that can help in tackling above mentioned challenges as the substrate properties play an important role in obtaining the effective implant-tissue interaction and osseointegration.

http://dx.doi.org/10.5772/66396

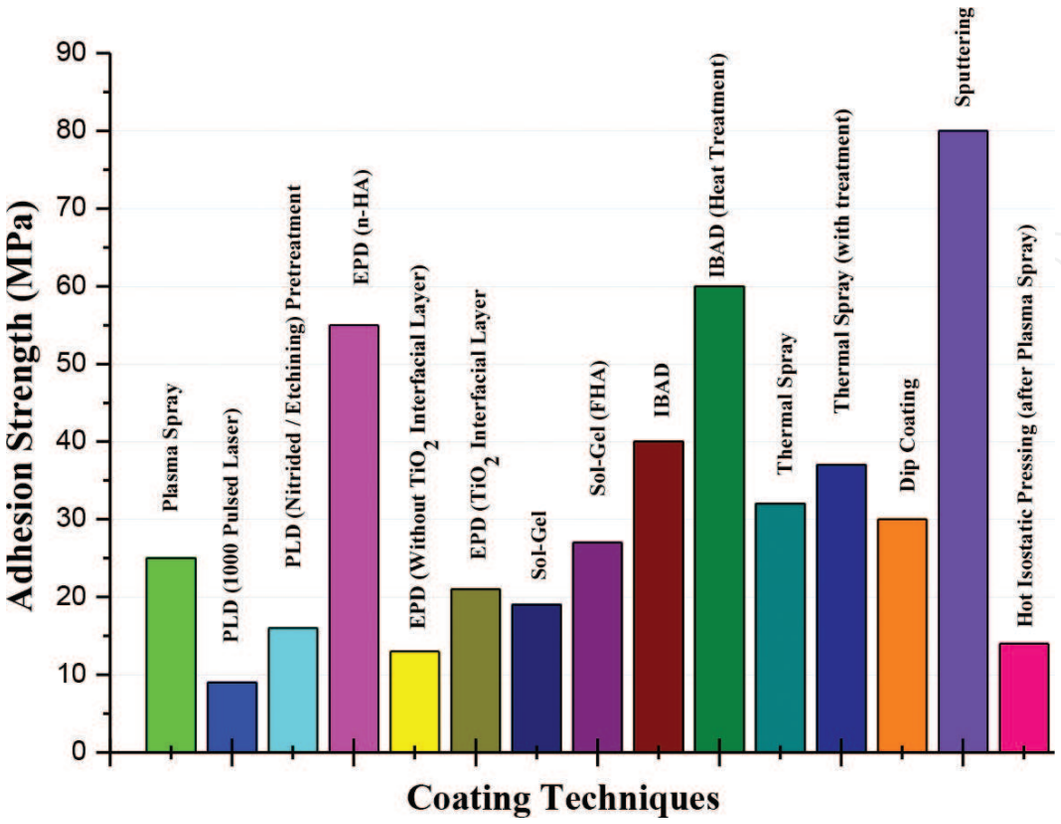

Figure 13. The quantitative comparison of different coating techniques. Reprinted from Mohseni et al. [81].

Substrate topography can be varied via different surface treatment procedures: exposition to abrasive paper (grinding and GR); sand, glass, or ceramic microspheres accelerated toward the surface (sandblasting and SB); exposition to acid chemicals (wet etching and AE); exposition to electron beams (EB). It is known that the mechanical properties of biomaterials are strongly governed by the film fabrication method and substrate characteristics. According to Mohseni et al. [81], the sputtering technique provides the highest adhesion of coating to the substrate compared to other methods which can be attributed to the sputter cleaning and ion bombardment processes (**Figure 13**). However, a simple and direct comparison of the effect of different pretreatment methods for enhancing the adhesion strength of magnetron sputtered HA coating is difficult because the deposition parameters are different and the authors use different techniques and experimental equipment to determine the mechanical properties. Nevertheless, the main tasks in the pretreatments of a metal surface prior to coating deposition may be defined as follows: to remove all foreign matter, to render surface suitable (suitable roughness) for the coating, to impart uniformity throughout all treated work piece surfaces.

Nowadays, the most common pretreatment methods of metallic substrate surface used prior to RF-magnetron coating deposition procedure are GR, SB, AE, and EB treatments [24, 56, 79, 81–84]. A number of studies reported that the combination of these pretreatment techniques

Sample	Substrate	*Thickness* (nm)	R_a (μm)	S_a, (nm)	h_c (nm)	*H* (GPa)	*E* (GPa)	*H*/*E*	H^3/E^2 (GPa)	Ref.
SB + AE + HA	Pure Ti (Grade 4)	500–800	0.8 ± 0.1		71.1 ± 2.9	15.2 ± 0.7	147 ± 16	0.101	164×10^{-3}	[85]
SB + AE + Ag - HA	Pure Ti (Grade 4)	450 ± 60	1.2 ± 0.1			2.8 ± 0.5	94 ± 24	0.030	2.4×10^{-3}	[87]
SB + AE + Ag - HA	Pure Ti (Grade 4)	450 ± 60	1.2 ± 0.1			5.3 ± 1.2	136 ± 28	0.039	7.8×10^{-3}	
HA	AZ31 magnesium alloy	700 ± 60			100	3.1 ± 2.0	79 ± 11	0.039	4.7×10^{-3}	[121]
					50	4.9 ± 2.5	78 ± 16	0.063	19.3×10^{-3}	
EB + HA	AZ31 magnesium alloy	700 ± 60			100	4.6 ± 0.8	63 ± 5	0.072	23.9×10^{-3}	
					50	8.5 ± 1.4	86 ± 5	0.099	82.9×10^{-3}	
AE + HA	Pure Ti (Grade 4)	500			100	3.8 ± 0.3	90 ± 8	0.047	6.6×10^{-3}	[83]
					50	3.6 ± 0.1	82 ± 10	0.047	6.9×10^{-3}	
AE + Ag - HA	Pure Ti (Grade 4)	500			100	7.2 ± 0.2	122 ± 4	0.060	25.1×10^{-3}	
					50	6.0 ± 0.5	96 ± 8	0.062	23.4×10^{-3}	
AE + HA	Pure Ti (Grade 4)	690 ± 125		50 ± 28	150 ± 10	3.7 ± 0.2	85 ± 10	0.043	7×10^{-3}	[56]
EB + HA	Pure Ti (Grade 4)	690 ± 125		21 ± 7	81 ± 4	7.0 ± 0.3	124 ± 3	0.056	22.3×10^{-3}	
GR + HA	NiTi and commercially pure Ti (Grade 4) i	90	<0.10		55 ± 15	11 ± 4	100 ± 20	0.110	133.1×10^{-3}	[24]
		270			165 ± 10	5 ± 1	100 ± 10	0.050	12.5×10^{-3}	
		450			202 ± 10	7 ± 2	100 ± 20	0.070	34.5×10^{-3}	
		720			150 ± 10	12 ± 2	130 ± 20	0.090	97.2×10^{-3}	
		1080			152 ± 20	13 ± 1	140 ± 10	0.090	112.1×10^{-3}	
		1600			130 ± 30	9 ± 1	111 ± 1	0.080	63.2×10^{-3}	
		2700			162 ± 10	9 ± 2	120 ± 20	0.080	50.6×10^{-3}	

Table 2. The most frequently applied pretreatment techniques prior the RF-magnetron sputtering and their influence on the mechanical characteristics of deposited HA-based coatings.

could be more effective for the improvement of hardness, Young's modulus and adhesion of the HA coatings to substrate [56, 85]. **Table 2** summarizes the use of different pretreatment methods prior the deposition of HA-based RF-magnetron coating on metallic substrate with comparison on their mechanical properties.

For instance, the increased surface roughness and enhanced mechanical properties of implants by SB and AE, so-called SLA process [86], were demonstrated by Grubova et al. [85]. Nanohardness H and Young's modulus E of the coatings prepared on Ti after SB with Al_2O_3 microspheres of 50 μm diameter followed the etching with a mixture of 1 ml HF + 2 ml HNO_3 + 2.5 ml H_2O at the penetration depth of hc = 71.11 ± 2.87 nm were 15.2 ± 0.7 and 147 ± 16 GPa, respectively. The values of H/E and H^3/E^2 for the HA coating (0.101 and 0.164 GPa, respectively) were significantly higher than that of the uncoated substrate (0.038 and 0.005 GPa). Scratch test results revealed that the deposited HA coatings exhibited improved wear resistance and lower friction coefficient. Eventually, the coating was delaminated from the substrate along the scratch path when the load increased up to 3.14 N.

Based on the data obtained in study [24] for pure HA coatings with a thickness of 0.09–2.7 μm prepared by RF-magnetron sputtering deposition on mechanically polished (GR) NiTi and Ti substrates at a substrate temperature of 500°C in argon atmosphere, we can assume that substrate surface microstructure affected the mechanical properties of HA films, if the film is thinner than about 1 μm. Their hardness and Young's modulus were of about 10 and 110 GPa, respectively. The bond strength of the HA coating to the metallic substrates is affected by its thickness. For example, upon increasing the thickness more than 1.6 μm, the bond strength decreased. The coating with a thickness of less than 1.6 μm was not damaged during the scratch test experiment even at a maximal load of 2 N. No difference was observed between NiTi and Ti substrates [24].

Control of the formation of the surface nanopatterns on Ti via pretreatments can allow varying the grain size of the HA coating. For instance, Grubova et al. [87] investigated the influence of the grain size on the mechanical properties of the nanostructured RF-magnetron sputter-deposited Ag-HA coatings with a concentration of silver in the range of 0.13–0.36 wt% prepared on the Ti substrates treated through SB with Al_2O_3 particles (250–320 μm) for 10 s at 0.45 and 0.61 MPa and AE using a 1:2:2.5 mixture of HF (40%), HNO_3 (66%), and distilled water. Larger nanostructure sizes were found on the surface of Ti prepared at a lower SB pressure. From the nanoindentation results, it is possible to conclude that smaller grains of the Ag-HA coatings resulted in significantly higher values of nanohardness and Young's modulus.

The treatment of Ti surfaces by EB has also been used prior the deposition of magnetron HA coatings [56]. EB irradiation of Ti samples has been found to reduce the roughness and to improve the nanohardness of the material [88], allowing for the deposition of smoother HA coatings [56]. For example, Surmeneva et al. [56] studied the nanoindentation hardness and the Young's modulus of the HA coating deposited onto Ti modified by the pulse EB treatment with an electron energy density of 15 J cm^{-2} were determined to be 7.0 ± 0.3 and 124 ± 3 GPa, respectively, which were significantly higher than those of the HA coating on AE Ti in a mixture of HF (48% concentration) and HNO_3 (65% concentration) acids; H_2O was set to 1:4:5 in volume. **Figure 14** shows the load-deformation curves of the tested in [56] surfaces.

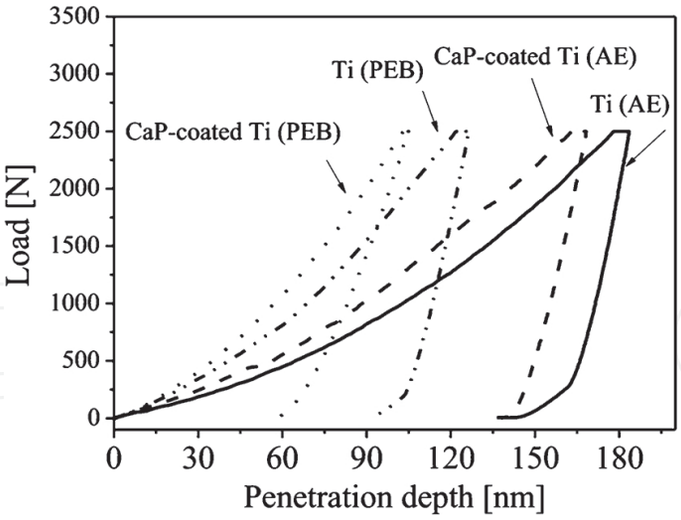

Figure 14. Representative load-displacement curves for uncoated and CaP—coated Ti prepared by AE and pulse EB treatment at a maximum load of 2.5 mN [56].

The CaP coating deposited onto the nanocrystalline EB treated Ti surface is more resistant to plastic deformation than the same coating on the AE Ti substrate. Moreover, Surmeneva et al. [89] also have evaluated the application of negative electrical bias to the Ti substrates preheated to $T = 200°C$ during the Si-HA coating deposition; the substrate surface was chemically etched and then treated with a low energy EB prior to deposition. It was found that for the case of the grounded substrate, the adhesion coefficient is the highest (HSC = 1). With increasing negative bias, the adhesion coefficient HSC lowers to 0.98, indicating a decrease in adhesion. Decreasing adhesion may be associated with an increasing level of microstrains because of a finer grained structure, an increasing volume fraction of defects, and incoherent interfaces, as evidenced by XRD and IR studies of the coating structures. Surmeneva et al.

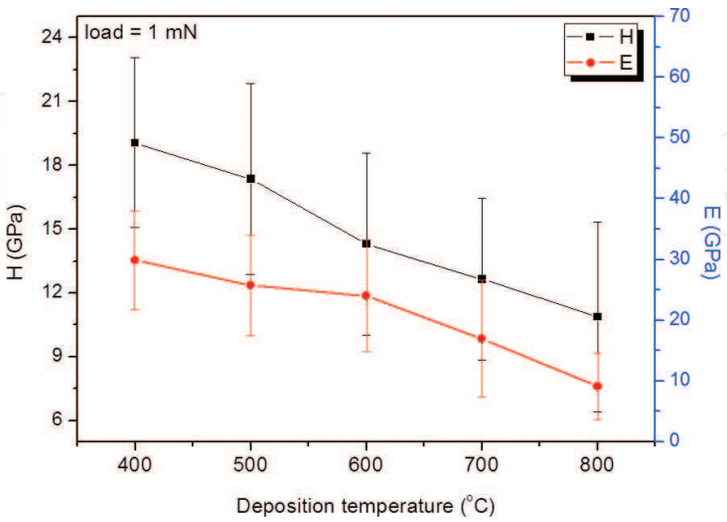

Figure 15. Hardness and elastic modulus of the sputtered CaP coatings prepared at different deposition temperatures; the measurements were performed on the coating deposited on the Si wafers in order to avoid the influence of other factors (e.g., roughness or cast defects occur during the deposition of the coatings on metallic substrates) [59].

found that the HA coating prepared on EB-treated magnesium AZ31 alloy exhibited higher hardness and the Young's modulus values compared to those of HA coated on untreated AZ 31 alloy. Furthermore, HA coating prepared on treated AZ31 alloy substrate showed the best resistance to plastic deformation than HA coated prepared on treated AZ31 alloy substrate. Although we cannot do the right comparison of the pretreatment methods usually used prior RF-magnetron coating deposition due to the differences in techniques and experimental equipment for the determination of the mechanical properties, we assume that pretreatments such as AE, SB, GR, and EB treatments and their combinations enhance the bonding strength and hardness of the coating. However, the pretreatments are not the only one way to guarantee a stable (high hardness and low friction) HA coating on metallic substrate. Using an interfacial layer (such as TiO_2, TiN, SiC, etc.) as the initial coating layer on the substrate followed by HA coating layer also can enhance the bonding strength and mechanical properties as well as post-treatments [84, 90–93].

In biomedical applications, the mechanical properties of the CaP coatings are important parameters. For success of dental or orthopedic implants, it is important to use a material with high hardness and elastic modulus close to the bone. In the case of CaP, both parameters are influenced by deposition temperature (**Figure 15**). Due to the plastic deformation, we presented the results of the hardness and elastic modulus measured at low load (1 mN). The elastic modulus and hardness values decreased with increasing deposition temperature (**Figure 15**). For both parameters, high values were obtained for the coatings with amorphous structure (sample deposited at 400°C). Note that the crystallinity plays an important role also in the case of mechanical properties. Despite that the high hardness is desired, the elastic modulus should be low, for the biomedical applications. Moreover, the CaP coatings exhibited a high dissolution rate in contact with human body fluids and it is not desired. Thus, the CaP coatings prepared at high deposition temperature (700 or 800°C) is more proper for coating the surface of dental or orthopedic implants.

2.8. Behavior *in vitro* of RF-magnetron sputtering of CaP coating

Cellular responses to an implanted biomaterial are highly complicated biological and chemical processes related to several surface properties [82]. In the literature, it was reported that the Ca and P content affected cell response such as attachment, spreading, and differentiation [61, 94–96]. Moreover, it was demonstrated that the biological properties of Ti or Mg alloys, ceramics, and polymers could be significantly enhanced by substrate coating with CaP thin film [61, 94–96].

In vitro cell viability tests studied after 5 days of culture with human osteosarcoma cell line (MG-63) showed that all of the cells have a good adhesion, spreading, and growth on the surface of all of the coatings, whatever deposition temperature was (**Figure 16**). Comparing all of the coatings, one may observe that there are no differences between the cell growths after increasing the deposition temperature. On all of the coated surfaces, the cells showed a dense cytoskeletal F-actin (stained green) and proliferated well, being situated close to each other. For the CaP coatings prepared at 700 and 800°C, more cell nuclei numbers (blue color) were found, indicating that these two coatings have better promoted the cell proliferation. The SEM micrograph of cell growth on the coating prepared at 800°C is presented in **Figure 17**. There

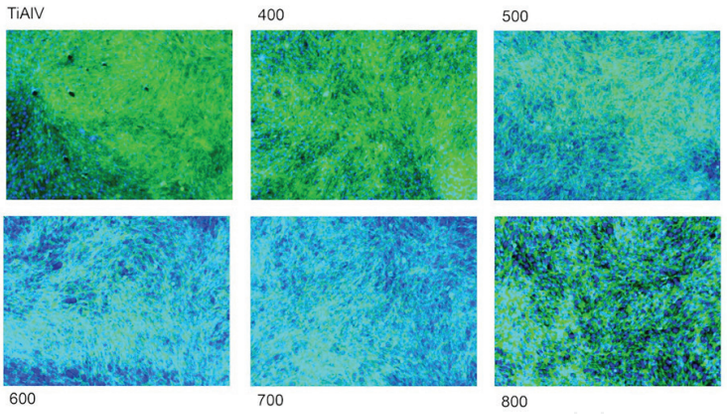

Figure 16. Fluorescence micrograph of the osteosarcoma cell growth after 5 days of culture on the uncoated Ti6Al4V substrate and coated at different deposition temperatures. Blue fluorescence represents the nuclei due to Hoechst 33342; green fluorescence is F-actin fibres due to FITC conjugated phalloidin [59].

are observed many cells well attached and spreading over the whole coated surface, with spindle-shaped, indicating good biocompatibility. In our previous paper, we demonstrated that this behavior was due to the increase of surface roughness which was increased due to the deposition temperature [59]. Immediately after the implantation, the first contact of the implant surface is with proteins, which are known as a promotor of attachments, spreading and proliferation of osteoblasts, leading to a successful implantation [97]. The proteins adhere better to the porous or rough surface due to larger contact areas which assure a bigger surface-cell interface [98, 99].

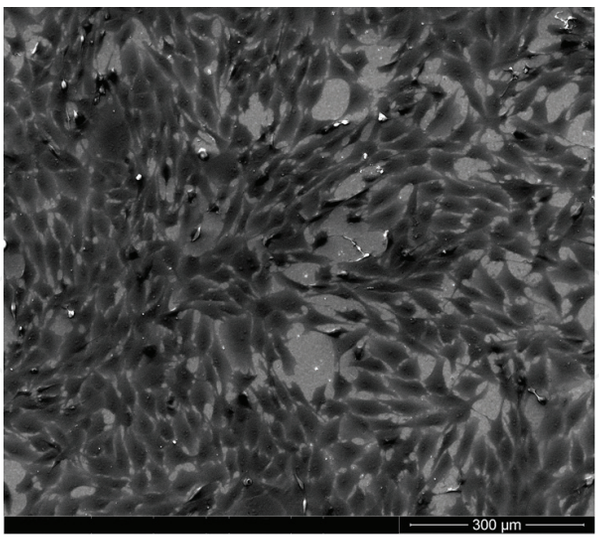

Figure 17. SEM image of the osteosarcoma cell growth after 5 days of culture on the coating prepared at 800°C.

Recent studies have shown that the cell-substrate interactions depend on the material type and are associated with the surface topography [100, 101], chemical and elemental composition [101, 102], dissolution behavior [101, 103], and surface macro and microstructure [101,

http://dx.doi.org/10.5772/66396

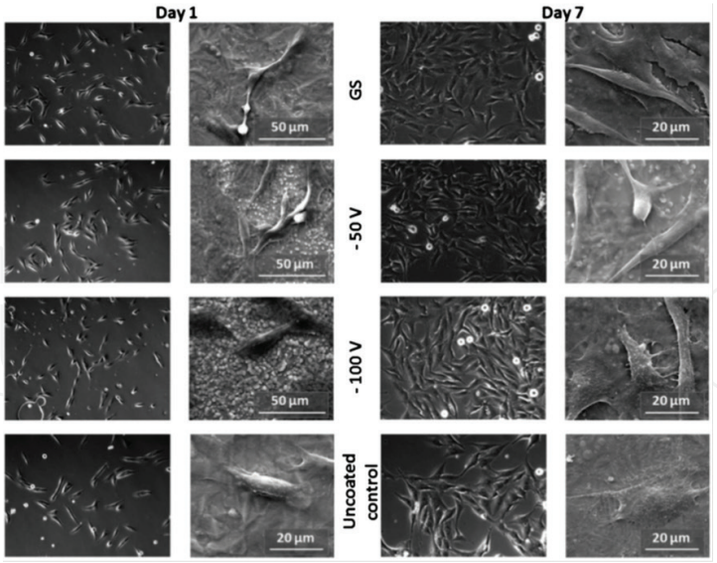

Figure 18. Morphology of MG-63 cells growth for 1 and 7 days on glass and Ti substrates coated with HA prepared by different methods [48].

104]. These physicochemical characteristics can be manipulated during RF-magnetron sputtering to promote the clinical integration of implants with the surrounding cells and tissue [100, 105]. The response of a human osteoblast-like cell line (MG-63) to titanium coated with silicon-containing calcium phosphate was investigated by Surmeneva et al [48]. *In vitro* cell culture studies showed that cells maintained their natural spindle-like morphology, are well spread out and adherent to the substrate (**Figure 18**). After 7 days, the cells covered the whole surface coated with HA. All the tested coatings revealed a low toxicity and a very good adhesion of cells on the surface.

By conducting the biological *in vitro* assay of the HA coatings with DPS cells the surface mineralization of the tested samples was revealed. The mineralized nodules typical for amorphous calcium phosphate (ACP) deposited from solutions were found in the extra-cellular region during the 3-day culture (**Figure 19a**) on the poor crystalline HA coating deposited at 200 W and 0.1 Pa on the titanium substrates. The calcification degree in the matrix of fibrous col-

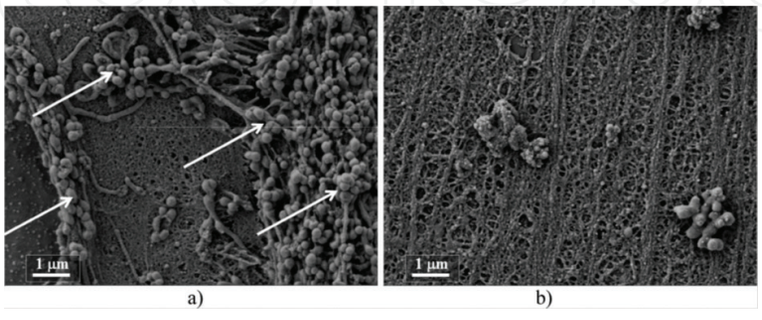

Figure 19. SEM image of the mineralized matrix synthesized by DPS cells cultured on the 440-nm thick CaP coating. The signs of mineralization are marked by arrows in (a). (b) Reveals the signs of mineralization in the case of uncoated titanium [52].

lagen was significantly lower in the case of the uncoated titanium (**Figure 19b**). It is reported that nodule formation in multilayers of cells is an important factor for *in vitro* mineralization [61, 62]. These results are consistence with those published in Ref. [63]. In the literature, it has been shown that the mineralization process is initiated by controlling the Ca and P concentrations in the medium [66, 68]. Nodule formation of mineralized is correlated with most of the biological events more or less with a spontaneous precipitation of CaP minerals, depending on the behavior of cellular osteogenic [69, 70]. In other words, poor crystalline HA coatings accelerated the attachment, proliferation, and formation of mineralized nodules by the cells grow on the surface than those grown on uncoated titanium surface.

The geometric and physical characteristics of the CaP film are important for regulation of the cells attachment and migration, such as crystallinity, composition, and thickness. Many scientific papers reported on the effect of crystalline and amorphous CaP coatings prepared by different techniques based on the adhesion, proliferation, and growth of bone-related cells [106–109]. Anyhow, most of the published papers acknowledged various effects of the CaP coating crystallinity on cell behavior. For example, a low dissolution rate of the coating was found for the coatings with low crystallinity or amorphous ones. On the other hand, the amorphous CaP coatings induce faster bone formation, even though its faster release of calcium ions [110]. Based on some *in vitro* analysis, it was found that the surface chemistry and topography of amorphous HA coatings stimulate the cell attachment, but result in a cytotoxic effect that inhibits proliferation of the cells attached to the coating surfaces [106, 110]. Simultaneously, highly crystalline HA coatings revealed nodule formation [106] and higher rates of osteogenic cell proliferation than the less crystalline or amorphous HA coatings deposited on Ti substrates [106, 110]. It is also reported in reference [107] that the amorphous sputtered CaP coatings constrain the growth and differentiation of rat bone marrow cells and osteoblast-like cells. On the other hand, crystalline HA coating prove to have better adhesion and accelerates proliferation of bone marrow mesenchymal stem cells compared with an amorphous ACP coating with the same topography and roughness [108].

It is difficult to highlight the most significant properties of the CaP coating that lead to a better cellular response. Furthermore, it is impossible to compare the results of *in vitro* experiments that have been conducted using different methodologies. For instance, the cell types influenced the Ca^{2+} and PO_4^{3-} and by varying the Ca/P ratio, the proliferation and differentiation could be controlled [111]. For this reason, the standardization to establish the effects of CaP on the biological assay is required. Up to date, there are some methodologies, but the published studies on the biological assay of the magnetron sputter-deposited coating demonstrate that this method can potentially be used for the development of future biomaterials.

3. Solutions for improving the properties of RF-magnetron sputtering of CaP coating

As it was underlined in the introduction, hydroxyapatite is one of the most extensively used materials in medicine for hard tissues repairment or for enhancing the osseointegration of

http://dx.doi.org/10.5772/66396

the metallic implants or their components. It is commonly used due to its chemical similarities to the component of bones and teeth. However, the high dissolution rate in contact with human fluids, the low mechanical strength and the relatively low bone bonding rate restrict its use as biomaterial. Therefore, the actual challenge in the biomedical field is to find a solution to improve the mentioned properties, but the difficulties are redoubtable, as these surface, characteristics deteriorate in time. A novel approach to obtain these surfaces is to modify HA properties by doping with small amounts of beneficial elements for human bones, as discuss below.

3.1. Si or SiC addition

In the present, the addition of Si into the HA matrix has successful clinic practice as bone graft material in spinal fusion (www.orthoaospl.com). However, this solution is not sufficient for the hard tissue, because they exhibited low hydrophobicity involves a decrease of the proteins adsorption and low mechanical and tribological properties. Thian et al. showed that sputtered Si-HA coatings could be a good candidate for hard tissue replacement, owing to their ability to form a carbonate-containing apatite layer rapidly [112]. Azem et al. showed that by SiC addition to the pure HA matrix, their corrosion resistance in artificial saliva and mechanical properties were enhanced, without affect the bioactive abilities of HA [91, 113]. Also, Vladescu et al. reported that the SiC consisting of hydroxyapatite coatings exhibited high adhesion strength to the Ti6Al4V substrates, better corrosion resistance to the SBF attack, better cells proliferation and viability compared with the undoped HA coatings. However, the elastic modulus is still higher than that of the bone [91].

3.2. Mg addition

Some researchers have also proposed the incorporation of Mg in the HA lattice, in order to accelerate the osseointegration process of dental or orthopedic implants. The Mg was selected as dopant because Mg is found in the natural dentin (1.23 wt%) and bone (0.73 wt%). However, a major drawback of the Mg-HA coatings is their high dissolution rate in physiological solutions, leading to a high pH value in the surrounding environment, which is detrimental to cell survival [114]. This effect appeared because Mg inhibits the apatite crystallization, leading to a destabilization of the apatite structure, by formation of the β-tricalcium phosphate, known as a phase with high dissolution rate in human body environment [113]. The 1.8 wt% Mg content decreased the compressive strength and hardness of the HA, but these are still higher than the values for bone [115].

3.3. Ti addition

A recent study reported that some of the properties of sputtered HA, such as mechanical properties, *in vitro* and *in vivo* bioactivity, could be enhanced by the incorporation of Ti in the HA lattice. Ribeiro et al. showed that the hydroxyapatite doped with Ti enhanced the protein adsorption, especially the activity of the enzyme GCR, indicating that this coatings may be used as a delivery matrix for biologically active molecules [116].

3.4. Ta addition

Ligot et al. identified that Ta could also be a promising doping element, proving that for Ta content less 4.5 at%, Ta substituted the Ca in the HA cell, and the (Ca + Ta)/P ratio is close to 1.67 (ratio of stoichiometric HA) and exhibited an elastic modulus of 120 GPa, which is comparable to the value of some conventional materials used for load-bearing implants (stainless steel, Co-Cr alloys or Ti alloys) for which the elastic modulus ranges between 110 and 232 GPa [117]. Unfortunately, up to date, no information about the effect of Ta addition on the osseointegration ability, bioactivity, or dissolution rate of sputtered HA coatings are available. Future work need to be done in this area.

3.5. Ag addition

In the present, in the biomedical applications, especially for dental and orthopedic implants, there is necessary to use surfaces with bioactive and antibacterial surfaces, which helps also the implant osseointegration. The bioactive surface could be achieved by using HA coatings, but the antibacterial or antifungal properties of HA coatings are under development. For example, Park et al. doped HA coatings with different Ag content and found that some of the Ca^{2+} ions in the hydroxyapatite were replaced with Ag^{+} ions [118]. The drawback of this solution is that the hardness and modulus of the Ag doped HA coatings decreased with an increasing Ag content [118], which is not desired for load bearing implants. Ciuca et al. found that the addition of 2.1 at.% Ag is enough for assuring of antifungal activity of the HA coating, without affecting the formation of the stoichiometric HA phase [119]. Also, it was demonstrated that the addition of a small Ag content (0.7 at.%) into HA structure could improve the resistance to the *Staphylococcus aureus*, *Streptococcus pyogenes*, *Salmonella typhimurium* attack of hydroxyapatite without any change of the other characteristics such as microchemical, microstructural, or anticorrosive ones of the sputtered hydroxyapatite [120].

4. Conclusions

The fabrication of a controlled crystallinity, chemistry, and stoichiometry of HA nanocoatings is shown to be possible based on the knowledge gained up to now, which will have a high efficiency in orthopedic implant applications. The HA coatings can be deposited on the surfaces of diverse metallic permanent and biodegradable implants. The complex geometries of implants can be coated by RF-magnetron sputter, even if this technique is a line-of-sight technique. An overall control of the coating properties keeping the adhesion strength to the substrate high makes RF-magnetron sputtering technique prospective for future commercial applications in the case of biocompatible coating fabrication.

Acknowledgements

This research was supported by the Federal Target Program #14.587.21.0013 (unique application number 2015-14-588-0002-5599), the Russian President grants MK-7907.2016.8, MK-6459.2016.8 and the State order NAUKA #11.1359.2014/K. The work was also supported by the grants of

the Romanian National Authority for Scientific Research and Innovation—UEFISCDI, Project numbers PN-II-PT-PCCA-2014-212, 44/2016 and 43/2016— INTELBIOCOMP, within PNCDI III and by the Core Program, under the support of ANCSI, project no. PN16.40.01.02.

Author details

Roman Surmenev[1], Alina Vladescu[1,2]*, Maria Surmeneva[1], Anna Ivanova[1], Mariana Braic[2], Irina Grubova[1] and Cosmin Mihai Cotrut[1,3]

*Address all correspondence to: alinava@inoe.ro

1 Tomsk Polytechnic University, Tomsk, Russia

2 National Institute for Research and Development in Optoelectronics, Bucharest, Romania

3 University Politehnica of Bucharest, Bucharest, Romania

References

[1] Surmenev RA, Surmeneva MA, Ivanova AA. Significance of calcium phosphate coatings for the enhancement of new bone osteogenesis—A review. Acta Biomater. 2014;10(2):557–579.

[2] Sobieszczyk S, Zieliński A. Coatings in arthroplasty: review paper. Adv Mater Sci. 2008;9:35–54.

[3] Liu D, Chou H, Wu J. Plasma-sprayed hydroxyapatite coating: effect of different calcium phosphate ceramics. J Mater Sci Mater [Internet]. 1994;147–153. Available from: http://link.springer.com/article/10.1007/BF00053335

[4] Yang Y, Kim KH, Ong JL. A review on calcium phosphate coatings produced using a sputtering process an alternative to plasma spraying. Biomaterials. 2005;26(3):327–337.

[5] Chu P. Plasma-surface modification of biomaterials. Mater Sci Eng R Reports. 2002;36(5–6):143–206.

[6] Zhang JX, Guan RF, Zhang XP. Synthesis and characterization of sol-gel hydroxyapatite coatings deposited on porous NiTi alloys. J Alloys Compd. 2011;509(13):4643–4648.

[7] Azem FA, Eroglu EO, Cakir A. Synthesis and structural properties of sol-gel derived Si-substituted hydroxyapatite coatings. J Biomech. 2011;44:13.

[8] Choi AH, Ben-Nissan B. Sol-gel production of bioactive nanocoatings for medical applications. Part II: current research and development. Nanomedicine (Lond). 2007;2(1):51–61.

[9] Eshtiagh-Hosseini H, Housaindokht MR, Chahkandi M. Effects of parameters of sol-gel process on the phase evolution of sol-gel derived hydroxyapatite. Mater Chem Phys. 2007;106:310–316.

[10] Liu DM, Troczynski T, Tseng WJ. Water-based sol-gel synthesis of hydroxyapatite: process development. Biomaterials. 2001;22(13):1721–30.

[11] Qu H, Wei M. Improvement of bonding strength between biomimetic apatite coating and substrate. J Biomed Mater Res - Part B Appl Biomater. 2008;84(2):436–443.

[12] Ballarre J, Seltzer R, Mendoza E, Orellano JC, Mai YW, García C, et al. Morphologic and nanomechanical characterization of bone tissue growth around bioactive sol-gel coatings containing wollastonite particles applied on stainless steel implants. Mater Sci Eng C. 2011;31(3):545–552.

[13] Rojaee R, Fathi M, Raeissi K, Sharifnabi A. Biodegradation assessment of nanostructured fluoridated hydroxyapatite coatings on biomedical grade magnesium alloy. Ceram Int. 2014;40(9):15149–15158.

[14] Olding T, Sayer M, Barrow D. Ceramic sol-gel composite coatings for electrical insulation. Thin Solid Films. 2001; 398–399:581–586.

[15] Cheang P, Khor KA. Addressing processing problems associated with plasma spraying of hydroxyapatite coatings. Biomaterials. 1996;17(5):537–544.

[16] Overgaard S, Soballe K, Josephsen K, Hansen ES, Bunger C. Role of different loading conditions on resorption of hydroxyapatite coating evaluated by histomorphometric and stereological methods. J Orthop Res. 1996;14(6):888–894.

[17] Vandijk K, Schaeken H, Wolke J, Jansen J. Influence of annealing temperature on RF magnetron sputtered calcium phosphate coatings. Biomaterials. 1996;17(4):405–410.

[18] Van Dijk K, Schaeken HG, Wolke JCG, Maree CHM, Habraken FHPM, Verhoeven J, et al. Influence of discharge power level on the properties of hydroxyapatite films deposited on Ti6A14V with RF magnetron sputtering. J Biomed Mater Res. 1995;29(2):269–276.

[19] Wolke JG, van Dijk K, Schaeken HG, de Groot K, Jansen JA. Study of the surface characteristics of magnetron-sputter calcium phosphate coatings. J Biomed Mater Res. 1994;28(12):1477–1484.

[20] Jansen JA, Wolke JG, Swann S, Van der Waerden JP, de Groot K. Application of magnetron sputtering for producing ceramic coatings on implant materials. Clin Oral Implants Res. 1993;4(1):28–34.

[21] Peter MM. Handbook of deposition technologies for films and coatings: Science, applications and technology. 3rd Edition. Andrew W, editor. Elsevier Inc, USA 2009. pp. 1–936.

[22] Yang J, Cui F, Lee IS, Wang X. Plasma surface modification of magnesium alloy for biomedical application. Surf Coat Technol. 2010;205:S182–S187.

[23] Paital SR, Dahotre NB. Calcium phosphate coatings for bio-implant applications: materials, performance factors, and methodologies. Mater Sci Eng R Reports. 2009.66: pp. 1–70.

[24] Pichugina VF, Surmeneva RA, Shesterikova EV, Ryabtsevaa MA, Eshenkoa EV, Tverdokhlebova SI, et al. The preparation of calcium phosphate coatings on titanium and nickel-titanium by rf-magnetron-sputtered deposition: composition, structure and micromechanical properties. Surf Coat Technol. 2008;202(16):3913–3920.

[25] Yeom GY, Thornton JA, Kushner MJ. Cylindrical magnetron discharges. II. The formation of dc bias in rf-driven discharge sources. J Appl Phys. 1989;65(10):3825–3832.

[26] Bikowski A, Welzel T, Ellmer K. The impact of negative oxygen ion bombardment on electronic and structural properties of magnetron sputtered ZnO: Al films. Appl Phys Lett. 2013;102(24):242106.

[27] Ellmer K, Welzel T. Reactive magnetron sputtering of transparent conductive oxide thin films: Role of energetic particle (ion) bombardment. J Mater Res. 2012;27(5):765–779.

[28] Ivanova AA, Surmeneva MA, Surmenev RA, Depla D. Influence of deposition conditions on the composition, texture and microstructure of rf-magnetron sputter-deposited hydroxyapatite thin films. In: Thin Solid Films. 2015. pp. 368–374.

[29] Tominaga K, Yuasa T, Kume M, Tada O. Influence of energetic oxygen bombardment on conductive ZnO films. Jpn J Appl Phys. 1985;24(8 R):944–949.

[30] Van Steenberge S, Leroy WP, Hubin A, Depla D. Momentum transfer driven textural changes of CeO_2 thin films. Appl Phys Lett. 2014;105(11):111602.

[31] Xu S, Long J, Sim L, Diong CH, Ostrikov K. RF plasma sputtering deposition of hydroxyapatite bioceramics: Synthesis, performance, and biocompatibility. Plasma Process Polym. 2005;2(5):373–390.

[32] Kester DJ, Messier R, Daniel J, Kestera. Macro-effects of resputtering due to negative ion bombardment of growing thin films. J Mater Res. 1993;8(8):1928–1937.

[33] Cuomo JJ, Gambino RJ, Harper JME, Kuptsis JD, Webber JC. Significance of negative ion formation in sputtering and SIMS analysis. J Vac Sci Technol. 1978;15(2):281.

[34] Cai Y, Liu W, He Q, Zhang Y, Yu T, Sun Y. Influence of negative ion resputtering on Al-doped ZnO thin films prepared by mid-frequency magnetron sputtering. Appl Surf Sci. 2010;256(6):1694–1697.

[35] Mattox DM. Particle bombardment effects on thin-film deposition: A review. J Vac Sci Technol A Vac Surf Film. 1989;7(3):1105–1114.

[36] Surmenev RA. A review of plasma-assisted methods for calcium phosphate-based coatings fabrication. Surf Coat Technol. 2012;206:2035–2056.

[37] Snyders R, Bousser E, Music D, Jensen J, Hocquet S, Schneider JM. Influence of the chemical composition on the phase constitution and the elastic properties of RF sputtered hydroxyapatite coatings. Plasma Process Polym. 2008;5(2):168–174.

[38] Snyders R, Music D, Sigumonrong D, Schelnberger B, Jensen J, Schneider JM. Experimental and ab initio study of the mechanical properties of hydroxyapatite. Appl Phys Lett. 2007;90(19):193902.

[39] Shi JZ, Chen CZ, Yu HJ, Zhang SJ. The effect of process conditions on the properties of bioactive films prepared by magnetron sputtering. Vacuum. 2008;83(2):249–256.

[40] Boyd AR, Meenan BJ, Leyland NS. Surface characterisation of the evolving nature of radio frequency (RF) magnetron sputter deposited calcium phosphate thin films after exposure to physiological solution. Surf Coat Technol. 2006;200(20–21):6002–6013.

[41] Boyd AR, Duffy H, McCann R, Cairns ML, Meenan BJ. The Influence of argon gas pressure on co-sputtered calcium phosphate thin films. Nucl Instrum Methods Phys Res Sect B Beam Interact Mater Atoms. 2007;258(2):421–428.

[42] Ozeki K, Goto T, Aoki H, Masuzawa T. Influence of the crystallinity of a sputtered hydroxyapatite film on its osteocompatibility. Biomed Mater Eng. 2015;26(3–4):139–147.

[43] Bramowicz M, Braic L, Azem FA, Kulesza S, Birlik I, Vladescu A. Mechanical properties and fractal analysis of the surface texture of sputtered hydroxyapatite coatings. Appl Surf Sci. 2016;379:338–346.

[44] López EO, Mello A, Farina M, Rossi AM, Rossi AL. Nanoscale analysis of calcium phosphate films obtained by RF magnetron sputtering during the initial stages of deposition. Surf Coat Technol. 2015;279:16–24.

[45] Surmeneva MA, Surmenev RA, Chaikina MV, Kachaev AA, Pichugin VF, Epple M. Phase and elemental composition of silicon-containing hydroxyapatite-based coatings fabricated by rf-magnetron sputtering for medical implants. Inorg Mater Appl Res. 2013;4(3):227–235.

[46] Surmenev RA, Ryabtseva MA, Shesterikov EV, Pichugin VF, Peitsch T, Epple M. The release of nickel from nickel-titanium (NiTi) is strongly reduced by a sub-micrometer thin layer of calcium phosphate deposited by rf-magnetron sputtering. J Mater Sci Mater Med. 2010;21(4):1233–1239.

[47] Surmeneva MA, Chaikina MV, Zaikovskiy VI, Pichugin VF, Buck V, Prymak O, et al. The structure of an rf-magnetron sputter-deposited silicate-containinghydroxyapatite-based coating investigated by high-resolution techniques. Surf Coat Technol. 2013;218(1):39–46.

[48] Surmeneva MA, Kovtun A, Peetsch A, Goroja SN, Sharonova AA, Pichugin VF, et al. Preparation of a silicate-containing hydroxyapatite-based coating by magnetron sputtering: structure and osteoblast-like MG63 cells in vitro study. RSC Adv. 2013;3:11240–112406.

[49] Krug J. Origins of scale invariance in growth processes. Adv Phys. 1997;46:139-282.

[50] Bales G, Zangwill A. Macroscopic model for columnar growth of amorphous films by sputter deposition. J Vac Sci Technol A. 1991;9(1):145–149.

[51] Ong JL, Harris LA, Lucas LC, Lacefield WR, Rigney D. X ray photoelectron spectroscopy characterization of ion beam sputter deposited calcium phosphate coatings. J Am Ceram Soc. 1991;74(9):2301–2304.

[52] Surmeneva MA, Surmenev RA, Nikonova YA, Selezneva II, Ivanova AA, Putlyaev VI, et al. Fabrication, ultra-structure characterization and in vitro studies of RF magnetron sputter deposited nano-hydroxyapatite thin films for biomedical applications. Appl Surf Sci. 2014;317:172–180.

[53] Wang X, Helmersson U, Madsen LD, Ivanov IP, Munger P, Rudner S, et al. Composition, structure, and dielectric tunability of epitaxial SrTiO3 thin films grown by radio frequency magnetron sputtering. J Vac Sci Technol VacSurf Film. 1999;17(2):564–570.

[54] Cuomo JJ, Rossnagel SM, Haufman HR, Komanduri R. Handbook of ion beam processing technology: principles, deposition, film modification, and synthesis. J Eng Mater Technol. 1990;112(2):253.

[55] Surmenev RA, Surmeneva MA, Evdokimov KE, Pichugin VF, Peitsch T, Epple M. The influence of the deposition parameters on the properties of an rf-magnetron-deposited nanostructured calcium phosphate coating and a possible growth mechanism. Surf Coat Technol. 2011;205(12):3600–3606.

[56] Surmeneva MA, Surmenev RA, Tyurin AI, Mukhametkaliyev TM, Teresov AD, Koval NN, et al. Comparative study of the radio-frequency magnetron sputter deposited CaP films fabricated onto acid-etched or pulsed electron beam-treated titanium. Thin Solid Films. 2014;571(P1):218–224.

[57] Feddes B, Wolke JGC, Jansen JA, Vredenberg AM. Radio frequency magnetron sputtering deposition of calcium phosphate coatings: The effect of resputtering on the coating composition. J Appl Phys. 2003;93:9503.

[58] Takayanagi S, Yanagitani T, Matsukawa M, Watanabe Y. Quantitative analysis of the effect of energetic particle bombardment during deposition on (1120) texture formation in ZnO films. In: IEEE International Ultrasonics Symposium. 2011. pp. 2317–2320.

[59] Vladescu A, Braic M, Azem FA, Titorencu I, Braic V, Pruna V, et al. Effect of the deposition temperature on corrosion resistance and biocompatibility of the hydroxyapatite coatings. Applied Surface Science. 2015;354:373–379.

[60] Xu L, Pan F, Yu G, Yang L, Zhang E, Yang K. In vitro and in vivo evaluation of the surface bioactivity of a calcium phosphate coated magnesium alloy. Biomaterials. 2009;30(8):1512–1523.

[61] Ueda K, Narushima T, Goto T, Taira M, Katsube T. Fabrication of calcium phosphate films for coating on titanium substrates heated up to 773 K by RF magnetron sputtering and their evaluations. Biomed Mater. 2007;2(3):S160–S166.

[62] Khor K, Dong Z, Quek C, Cheang P. Microstructure investigation of plasma sprayed HA/Ti6Al4V composites by TEM. Mater Sci Eng A. 2000;281(1–2):221–228.

[63] Dong Z, Khor K, Quek C, White T, Cheang P. TEM and STEM analysis on heat-treated and in vitro plasma-sprayed hydroxyapatite/Ti-6Al-4V composite coatings. Biomaterials. 2003;24(1):97–105.

[64] Karunasiri RPU, Bruinsma R, Rudnick J. Thin-film growth and the shadow instability. Phys Rev Lett. 1989;62(7):788–791.

[65] Mahieu S, Ghekiere P, Depla D, De Gryse R. Biaxial alignment in sputter deposited thin films.Thin Solid Films. 2006;515:1229–1249.

[66] Mahieu S, Depla D. Reactive sputter deposition of TiN layers: modelling the growth by characterization of particle fluxes towards the substrate. J Phys D Appl Phys. 2009;42(5):53002.

[67] Mahieu S, Leroy WP, Van Aeken K, Depla D. Modeling the flux of high energy negative ions during reactive magnetron sputtering. J Appl Phys. 2009;106(9):093302.

[68] Filgueiras MRT, Mkhonto D, Leeuw NH. Computer simulations of the adsorption of citric acid at hydroxyapatite surfaces. J Cryst Growth. 2006;294(1):60–68.

[69] Van Steenberge S, Leroy WP, Depla D. Influence of oxygen flow and film thickness on the texture and microstructure of sputtered ceria thin films. Thin Solid Films. 2014;553:2–6.

[70] Hong RJ, Helming K, Jiang X, Szyszka B. Texture analysis of Al-doped ZnO thin films prepared by in-line reactive MF magnetron sputtering. Appl Surf Sci. 2004;226(4):378–86.

[71] Lee YE, Lee J Bin, Kim YJ, Yang HK, Park JC, Kim HJ. Microstructural evolution and preferred orientation change of radio-frequency-magnetron sputtered ZnO thin films. J Vac Sci Technol A. 1996;14(3):1943–1998.

[72] Dong XL, Zhou HL, Wu T, Wang Q. Behavior regulation of adsorbed proteins via hydroxyapatite surface texture control. J Phys Chem B. 2008;112(15):4751–4759.

[73] Kim H, Camata RP, Chowdhury S, Vohra YK. In vitro dissolution and mechanical behavior of c-axis preferentially oriented hydroxyapatite thin films fabricated by pulsed laser deposition. Acta Biomater. 2010;6(8):3234–3241.

[74] Oonishi H. Orthopaedic applications of hydroxyapatite. Biomaterials. 1991;12(2):171–178.

[75] Zhuang Z, Fujimi TJ, Nakamura M, Konishi T, Yoshimura H, Aizawa M. Development of a,b-plane-oriented hydroxyapatite ceramics as models for living bones and their cell adhesion behavior. Acta Biomater. 2013;9(5):6732–6740.

[76] Wenk HR, Heidelbach F. Crystal alignment of carbonated apatite in bone and calcified tend on: results from quantitative texture analysis. Bone. 1999;24(4):361–369.

[77] Nakano T, Kaibara K, Tabata Y, Nagata N, Enomoto S, Marukawa E, et al. Unique alignment and texture of biological apatite crystallites in typical calcified tissues analyzed by microbeam x-ray diffractometer system. Bone. 2002;31(4):479–487.

[78] Radin SR, Ducheyne P. The effect of calcium phosphate ceramic composition and structure on in vitro behavior. II. Precipitation. J Biomed Mater Res. 1993;27(1):35–45.

[79] Baboian R. Corrosion tests and standards: application and interpretation. 2nd Edition. ASTM International, Philadelphia, USA; 2005. 867 p.

[80] Mansfeld F. The Polarization Resistance Technique for Measuring Corrosion Currents. In: Fontana, Mars G., Staehle RW, editor. Advances in Corrosion Science and Technology Springer US, New York. 1976;6:pp. 163–262.

[81] Mohseni E, Zalnezhad E, Bushroa AR. Comparative investigation on the adhesion of hydroxyapatite coating on Ti–6Al–4V implant: a review paper. Int J Adhes Adhes. 2014;48:238–257.

[82] Ozeki K, Fukui Y, Aoki H. Hydroxyapatite coated dental implants by sputtering technique. Biocybern Biomed Eng. 2006;26(1):95–101.

[83] Ivanova AA, Surmeneva MA, Tyurin AI, Pirozhkova TS, Shuvarin IA, Prymak O, et al. Fabrication and physico-mechanical properties of thin magnetron sputter deposited silver-containing hydroxyapatite films. Appl Surf Sci. 2016;360:929–935.

[84] Nelea V, Morosanu C, Iliescu M, Mihailescu IN. Microstructure and mechanical properties of hydroxyapatite thin films grown by RF magnetron sputtering. Surf Coat Technol. 2003;173(2–3):315–322.

[85] Grubova I, Priamushko T, Chudinova E, Surmeneva M, Korneva O, Epple M, et al. Formation and characterization of crystalline hydroxyapatite coating with the (002) texture. In: IOP Conf Ser Mater Sci Eng. 2016. p. 12016.

[86] Buser D, Schenk RK, Steinemann S, Fiorellini JP, Fox CH, Stich H. Influence of surface characteristics on bone integration of titanium implants. A histomorphometric study in miniature pigs. J Biomed Mater Res. 1991;25(7):889–902.

[87] Grubova IY, Surmeneva MA, Ivanova AA, Kravchuk K, Prymak O, Epple M, et al. The effect of patterned titanium substrates on the properties of silver-doped hydroxyapatite coatings. Surf Coat Technol. 2015;276:595–601.

[88] Gao Y. Surface modification of TA2 pure titanium by low energy high current pulsed electron beam treatments. Appl Surf Sci. 2011;257(17):7455–7460.

[89] Surmeneva MA, Surmenev RA, Pichugin VF, Koval' NN, Teresov AD, Ivanova AA, et al. Adhesion properties of a silicon-containing calcium phosphate coating deposited by RF magnetron sputtering on a heated substrate. J Surf Invest X-ray, Synchrotron Neutron Tech. 2013;7(5):944–951.

[90] Brossa F, Cigada A, Chiesa R, Paracchini L, Consonni C. Post-deposition treatment effects on hydroxyapatite vacuum plasma spray coatings. J Mater Sci Mater Med. 1994;5(12):855–857.

[91] Vladescu A, Birlik I, Braic V, Toparli M, Celik E, Ak Azem F. Enhancement of the mechanical properties of hydroxyapatite by SiC addition. J Mech Behav Biomed Mater. 2014;40:362–368.

[92] Azem FA, Birlik I, Braic V, Toparli M, Celik E, Parau A, et al. Effect of SiC interlayer between Ti6Al4V alloy and hydroxyapatite films. Proc Inst Mech Eng Part H J Eng Med. 2015;229(4):307–318.

[93] Nelea V, Morosanu C, Iliescu M, Mihailescu IN. Hydroxyapatite thin films grown by pulsed laser deposition and radio-frequency magnetron sputtering: comparative study. Appl Surf Sci. 2004;228(1–4):346–536.

[94] Feng B, Weng J, Yang BC, Qu SX, Zhang XD. Characterization of titanium surfaces with calcium and phosphate and osteoblast adhesion. Biomaterials. 2004;25(17):3421–3428.

[95] Pisarek M, Roguska A, Andrzejczuk M, Marcon L, Szunerits S, Lewandowska M, et al. Effect of two-step functionalization of Ti by chemical processes on protein adsorption. Appl Surf Sci. 2011;257(19):8196–8204.

[96] Schade R, Sikiri MD, Lamolle S, Ronold HJ, Lyngstadass SP, Liefeith K, et al. Biomimetic organic-inorganic nanocomposite coatings for titanium implants. in vitro and in vivo biological testing. J Biomed Mater Res - Part A. 2010;95(3 A):691–700.

[97] Andrade J, Hlady V, Feng L, Tingey K. Proteins at interfaces: principles, problems, and potential. In: Bioprocess Technology. Dekker, New York 1996. pp. 19–55.

[98] Woo KM, Chen VJ, Ma PX. Nano-fibrous scaffolding architecture selectively enhances protein adsorption contributing to cell attachment. J Biomed Mater Res A. 2003;67:531–537.

[99] Webster TJ, Ergun C, Doremus RH, Siegel RW, Bizios R. Specific proteins mediate enhanced osteoblast adhesion on nanophase ceramics. J Biomed Mater Res. 2000;51(3):475–483.

[100] Yang SP, Yang CY, Lee TM, Lui TS. Effects of calcium-phosphate topography on osteoblast mechanobiology determined using a cytodetacher. Mater Sci Eng C. 2012;32(2):254–262.

[101] Chai YC, Truscello S, Bael S Van, Luyten FP, Vleugels J, Schrooten J. Perfusion electrodeposition of calcium phosphate on additive manufactured titanium scaffolds for bone engineering. Acta Biomater. 2011;7(5):2310–2319.

[102] Habibovic P, Kruyt MC, Juhl MV, Clyens S, Martinetti R, Dolcini L, et al. Comparative in vivo study of six hydroxyapatite-based bone graft substitutes. J Orthop Res. 2008;26(10):1363–1370.

[103] Becker P, Neumann HG, Nebe B, Lüthen F, Rychly J. Cellular investigations on electrochemically deposited calcium phosphate composites.J Mater Sci Mater in Med. 2004;15: 437–440.

[104] Yuan H, Kurashina K, De Bruijn JD, Li Y, De Groot K, Zhang X. A preliminary study on osteoinduction of two kinds of calcium phosphate ceramics. Biomaterials. 1999;20(19):1799–1806.

[105] Yu S, Yu Z, Wang G, Han J, Ma X, Dargusch MS. Biocompatibility and osteoconduction of active porous calcium-phosphate films on a novel Ti-3Zr-2Sn-3Mo-25Nb biomedical alloy. Colloids and Surf B Biointerfaces. 2011; 85:103–115.

[106] Berube P, Yang Y, Carnes DL, Stover RE, Boland EJ, Ong JL. The effect of sputtered calcium phosphate coatings of different crystallinity on osteoblast differentiation. J Periodontol. 2005;76(10):1697–1709.

[107] Brugge, Ter PJ, Wolke JG, Jansen JA. Effect of calcium phosphate coating composition and crystallinity on the response of osteogenic cells in vitro. Clin Oral Implants Res. 2003;14(4):472–480.

[108] Hu Q, Tan Z, Liu Y, Tao J, Cai Y, Zhang M, et al. Effect of crystallinity of calcium phosphate nanoparticles on adhesion, proliferation, and differentiation of bone marrow mesenchymal stem cells. J Mater Chem. 2007;17(44):4690.

[109] Siebers MC, Walboomers XF, Leeuwenburgh SCG, Wolke JGC, Jansen JA. The influence of the crystallinity of electrostatic spray deposition-derived coatings on osteoblast-like cell behavior, in vitro. J Biomed Mater Res—Part A. 2006;78(2):258–267.

[110] Chou L, Marek B, Wagner WR. Effects of hydroxylapatite coating crystallinity on biosolubility, cell attachment efficiency and proliferation in vitro. Biomaterials. 1999;20(10):977–985.

[111] Barrère F, van Blitterswijk CA, de Groot K. Bone regeneration: molecular and cellular interactions with calcium phosphate ceramics. IntJ Nanomed. 2006;1:317–332.

[112] Thian ES, Huang J, Best SM, Barber ZH, Bonfield W. Novel silicon-doped hydroxyapatite (Si-HA) for biomedical coatings: An in vitro study using a cellular simulated body fluid. J Biomed Mater Res - Part B Appl Biomater. 2006;76(2):326–333.

[113] Azem FA, Kiss A, Birlik I, Braic V, Luculescu C, Vladescu A. The corrosion and bioactivity behavior of SiC doped hydroxyapatite for dental applications. Ceram Int. 2014;40(10):15881–15887.

[114] Šupová M. Substituted hydroxyapatites for biomedical applications: a review. Ceram Int. 2015;41(8):9203–9231.

[115] Zyman Z, Tkachenko M, Epple M, Polyakov M, Naboka M. Magnesium-substituted hydroxyapatite ceramics. Materwiss Werksttech. 2006;37(6):474–477.

[116] Ribeiro AR, Piedade AP, Ribeiro CC, Vieira MT, Barbosa MA. Characterization of hydroxyapatite sputtered films doped with titanium. Key Eng Mater. 2007;330–332:649–652.

[117] Ligot S, Godfroid T, Music D, Bousser E, Schneider JM, Snyders R. Tantalum-doped hydroxyapatite thin films: Synthesis and characterization. Acta Mater. 2012;60(8):3435–3443.

[118] Park SS, Lee HJ, Oh IH, Lee BT. Effects of Ag-doping on microstructure and mechanical properties of hydroxyapatite films. Key Eng Mater. 2005;277–279:113–8.

[119] Ciuca S, Badea M, Pozna E, Pana I, Kiss A, Floroian L, et al. Evaluation of Ag containing hydroxyapatite coatings to the *Candida albicans* infection. J Microbiol Methods. 2016;125:12–18.

[120] Badea M, Braic M, Kiss A, Moga M, Pozna E, Pana I, et al. Influence of Ag content on the antibacterial properties of SiC doped hydroxyapatite coatings. Ceram Int. 2016;42(1):1801–1811.

[121] Surmeneva MA, Tyurin AI, Teresov AD, Koval NN, Pirozhkova TS, Shuvarin IA, et al. Combined effect of pulse electron beam treatment and thin hydroxyapatite film on mechanical features of biodegradable AZ31 magnesium alloy. IOP Conf Ser Mater Sci Eng. 2015;98:12030.